

Optimization of Efficiency and Energy Consumption in p -Persistent CSMA-Based Wireless LANs

Raffaele Bruno, Marco Conti, *Member, IEEE*, and Enrico Gregori, *Member, IEEE*

Abstract—Wireless technologies in the LAN environment are becoming increasingly important. The IEEE 802.11 is the most mature technology for Wireless Local Area Networks (WLANs). The limited bandwidth and the finite battery power of mobile computers represent one of the greatest limitations of current WLANs. In this paper, we deeply investigate the efficiency and the energy consumption of MAC protocols that can be described with a p -persistent CSMA model. As already shown in the literature, the IEEE 802.11 protocol performance can be studied using a p -persistent CSMA model [12]. For this class of protocols, in the paper, we define an analytical framework to study the theoretical performance bounds from the throughput and the energy consumption standpoint. Specifically, we derive the p values (i.e., the average size of the contention window in the IEEE 802.11 protocol [12]) that maximizes the throughput, p_{opt}^C , and minimizes the energy consumption, p_{opt}^E . By providing analytical closed formulas for the optimal p values, we discuss the trade-off between efficiency and energy consumption. Specifically, we show that power saving and throughput maximization can be jointly achieved. Our analytical formulas indicate that the optimal p values depend on the network configuration, i.e., number of active stations and length of the messages transmitted on the channel. As network configurations dynamically change, the optimal p values must be dynamically updated. In this paper, we propose and evaluate a simple but effective feedback-based distributed algorithm for tuning the p parameter to the optimal values, i.e., p_{opt}^E and p_{opt}^C . The performance of the p -persistent IEEE 802.11 protocol, enhanced with our algorithm, are extensively investigated by simulation. Our results indicate that the enhanced p -persistent IEEE 802.11 protocol is very close to the theoretical bounds both in steady-state and in transient conditions.

Index Terms—Wireless LAN (WLAN), IEEE 802.11, random access protocol, performance analysis, energy consumption, protocol capacity.

1 INTRODUCTION

IN the recent years, the proliferation of portable computers, handheld digital devices, and PDAs has led to a rapid growth in the use of wireless technologies for the Local Area Network (LAN) environment. Beyond supporting wireless connectivity for fixed, portable, and moving stations within a local area, the wireless LAN (WLAN) technologies can provide a mobile and ubiquitous connection to the Internet information services. Hence, it is foreseeable that, in the not-so-distant future, the WLAN technologies will become more and more used as means to access the Internet. Wireless communications and the mobile nature of devices involved in constructing WLANs generate new research issues compared with wired networks: dynamic topologies, limited bandwidth, energy-constrained operations, and noisy channel. Because nodes can move arbitrarily, the network configuration can change randomly and rapidly. This means that the number of mobile hosts belonging to the same WLAN can be highly variable. The design of WLANs has to concentrate on bandwidth consumption because wireless networks deliver much lower bandwidth than wired networks, e.g., 2-11 Mbps

versus 10-150 Mbps [32]. Furthermore, the finite battery power of mobile computers represents one of the greatest limitations to the utility of portable computers [37]. Specifically, for these devices, the finite battery power represents a severe limitation because the data transmission and reception are one of the most power-consuming activities that these devices have to perform [1]. Due to technology limitations, it is extremely difficult to significantly increase the battery capacity; hence, it is vital to manage efficiently the power utilization by identifying any way to use less power preferably without negatively impacting the channel utilization. The power saving features of the emerging standards for WLANs have been analyzed in [37], [15], [24].

The most mature technology is the one defined by the IEEE 802.11 standard [28] which follows the Carrier Sensing Multiple Access with Collision Avoidance (CSMA/CA) paradigm. For this reason, in this paper, we will use the IEEE 802.11 technology as the reference point.

In WLANs, the Medium Access Control (MAC) protocol is the main element that determines the efficiency in sharing the limited resources of the wireless channel since it performs the coordination of transmissions of the network stations. At the same time, the MAC protocol manages the congestion situations that may occur inside the network. The congestion level in the network negatively affects both the channel utilization (i.e., the fraction of channel bandwidth used from successfully transmitted messages) and the energy consumed to successfully transmit a message. Specifically, each collision removes both the channel bandwidth and the battery capacity from that

• The authors are with Istituto CNUCE, Consiglio Nazionale delle Ricerche, Vis G. Moruzzi, 1, 56124 Pisa, Italy.
E-mail: Raffaele.Bruno@guest.cnuce.cnr.it and [Marco.Conti, Enrico.Gregori]@cnuce.cnr.it.

Manuscript received 11 Feb. 2001; revised 22 Nov. 2001; accepted 25 Feb. 2002.

For information on obtaining reprints of this article, please send e-mail to: tmc@computer.org, and reference IEEECS Log Number 9-022002.

available for successful transmissions. To reduce the collision probability, the IEEE 802.11 protocol uses a set of slotted windows for the backoff whose size doubles after each collision. However, the time spreading of the accesses that the standard backoff procedure accomplishes can have a negative impact on both the channel utilization and the energy consumption. Specifically, the time spreading of the accesses can introduce channel idle periods and, hence, additional energy wastage due to the carrier sensing. Furthermore, this policy has to pay the cost of collisions to increase the backoff time when the network is congested. Several solutions have been proposed to improve the efficiency of IEEE 802.11 ([36], [12], [13], [3], [30], [8], and [7]). Specifically, [12], [13], [5] proposed to dynamically control the network congestion by investigating the number of users in the system. This investigation could be expensive, difficult to obtain, and subject to significant errors, especially in high contention situations [13]. Distributed strategies for power saving were proposed in ([30] and [8]). Bononi et al. [8] extend the algorithm presented in [7] with power saving features. Finally, [36] and [7] proposed solutions to have a more uniform distribution of channel accesses.

Most of the IEEE 802.11 results are obtained using the *p-persistent* model of the IEEE 802.11 protocol ([12], [5], [4], [6], [8], [34]). This model differs from the standard protocol only in the selection of the backoff interval. Instead of the binary exponential backoff used in the standard, the backoff interval of the *p-persistent* IEEE 802.11 protocol is sampled from a geometric distribution with parameter p . A *p-persistent* IEEE 802.11 closely approximates the standard protocol if the p value is selected to guarantee that the same average backoff interval is used in the two protocols [12]. Due to its memoryless backoff algorithm, the *p-persistent* IEEE 802.11 protocol is suitable for analytical studies.

In this paper, we develop a general analytical framework to study both the channel utilization and energy consumption for a large class of MAC protocol for WLANs, i.e., those adopting *p-persistent* CSMA/CA MAC protocol. Our framework includes the *p-persistent* IEEE 802.11 as a special case. By exploiting our analytical model, we will derive the theoretical bounds for both the channel utilization and the energy consumption. Specifically, we derive analytical formulas for the protocol capacity and the energy consumption. From these formulas, we compute the p value corresponding to the maximum channel utilization (*optimal capacity* p , also referred to as p_{opt}^C), and the p value corresponding to the minimum energy consumption (*optimal energy* p , also referred to as p_{opt}^E). The properties of the optimal operating points are deeply investigated in the paper. In addition, we also provide closed formulas for the optimal p values. These formulas can be used to tune a WLAN network either to maximize its efficiency or to minimize its energy consumption. Furthermore, from our analysis, we have discovered that, for the system-parameter values typical of current WLANs ([35], [24]), power saving and maximum throughput are not orthogonal targets, i.e., the p value that optimizes one performance figure provides a quasi-optimal value also for the other performance figure.

The tuning of a WLAN by adopting the closed formulas developed in the paper requires an a priori knowledge of the network configuration, i.e., the number of active stations in the network and the message length characteristics. Unfortunately, in a real case, a station does not have an

exact knowledge of the network configuration, but it can (at most) estimate it by observing the channel status. Hence, in this paper, we propose and validate a novel algorithm that, by adopting a feedback from the channel status and our analytical formulas, tunes the value of the p parameter. Our feedback-based algorithm is used to enhance the *p-persistent* IEEE 802.11 protocol. Via simulation, we have compared the performance figures of the *p-persistent* IEEE 802.11 protocol with or without our feedback-based algorithm. Results obtained indicate that under *stationary* traffic and network configurations (i.e., constant average message length and fixed number of active stations) the enhanced protocol significantly improves the standard protocol and (in all the configurations analyzed) it always reaches the theoretical limits. In addition, we investigate the protocol performance in *transient conditions* (i.e., when the number of active stations changes). Results indicate the promptness of the enhanced protocol to retune its p parameter to the new optimal value also when the network state changes. Finally, we show that the feedback-based algorithm does not introduce any additional delay in accessing the network.

The paper is organized as follows: Section 2 presents our system model. Section 3 presents an exhaustive analysis of the efficiency and energy consumption for *p-persistent* CSMA access schemes. In Section 4, we define our novel transmission control strategy. In Section 5, we extend the *p-persistent* IEEE 802.11 with the proposed feedback-based tuning algorithm. Concluding remarks are summarized in Section 5.

2 MODELING *p-PERSISTENT* CSMA ACCESS SCHEMES

The performances of *p-persistent* CSMA protocols were investigated in depth by Kleinrock and Tobagi in [26]. Their analytical model adopts an infinite population model and assumes that the backlog has a Poisson distribution. The Poisson model is an approximation to a large but finite population in which each station generates messages infrequently and each message can be successfully transmitted in a time interval much shorter than the average time between successive messages generated by a given station. The current usage scenarios for the wireless local area networks impose to do not consider anymore the networks as lightly loaded and each station as a source of sparse messages. These considerations motivate the need to study the network behavior by assuming a system with a finite number M of active stations in which each station may generate a significant portion of the network traffic. To represent a realistic WLAN environment, in our study, M is in the range $[2, \dots, 100]$.

To be as general as possible, we model a family of random access schemes. Specifically, we assume a slotted multiple-access channel and the random access protocols can be either a Slotted-ALOHA or a *p-persistent* CSMA algorithm [2]. In this way, we obtain results that apply to a large class of random access protocols. Note that *p-persistent* IEEE 802.11 can be considered as a special case of this family [12]. In Section 5, these general results are applied to the *p-persistent* IEEE 802.11 case. In our model, the channel idle time is divided into fixed length intervals. Hereafter, we refer to each time interval as a time slot, say t_{slot} . All stations in the network are synchronized and are forced to start a transmission only at the beginning of a time slot.

In the Slotted-ALOHA case, the stations transmit constant-length messages with length l that exactly fits in a slot. In the CSMA case, the message length is a random variable L , with average l . Hereafter, to simplify the presentation, we will assume that L values always correspond to an integer number of slots. For this reason, in this paper, the message lengths are normalized with respect to the slot length.

When a station has a new message to transmit, it senses the channel if it is idle, then it transmits the message with probability p , while with probability $1 - p$, it delays the message transmission to the next time slot. On the other hand, if a station with a new message to transmit senses the channel is busy, the message is regarded as backlogged and the station will attempt the message transmission in the next empty slot with probability p . After a collision, the collided message transmission is rescheduled immediately according to the same rules adopted for the newly generated messages.

In our protocol model, we assume that the acknowledgements are instantaneously received and do not occupy any channel time (for instance, the acknowledgement information could be delivered by out-of-band signaling). This assumption is adopted for the sake of generalization in the protocol analysis. The acknowledgements only introduce a fixed overhead, but they do not have a significant impact on the protocol behavior. Therefore, this assumption is usually adopted in any performance analysis of random access protocols [26], [22]. It is worth pointing out that the acknowledgements will be taken into consideration when the p -persistent IEEE 802.11 MAC protocol is considered, see Section 5.

The aim of this paper is to study the **EFFICIENCY** and **ENERGY CONSUMPTION** of p -persistent CSMA Access Schemes and to apply the results of this study to optimize the performance of the p -persistent IEEE 802.11 MAC protocol.

EFFICIENCY. The fraction of channel bandwidth used by successfully transmitted messages gives a good indication of the overheads required by the MAC protocol to perform its coordination task among stations. This fraction is known as the channel utilization. Hereafter, ρ will denote the channel utilization. The maximum value it can attain, named MAC protocol *capacity* [16], is the best figure to express the efficiency of a WLAN technology. Hereafter, ρ_{MAX} will denote the MAC protocol *capacity*.

ENERGY CONSUMPTION. The finite battery power represents the other greatest limitation to the utility of portable computers [14], [18], [29]. The network interface is one of the main system components from the battery consumption standpoint [27]. Hence, the energy used by the network interface to successfully transmit a message is the other important figure for a mobile computer. To express this important figure, in this paper, we introduce the index ρ_{energy} to measure the energy efficiency of a protocol. The exact definition of this index is reported in (5) below.

To derive a closed formula for ρ and ρ_{energy} in the paper, we assume that: 1) All the network active stations operate in *asymptotic conditions*, i.e., they always have a message waiting to be transmitted. 2) The message lengths (expressed as the number of consecutive t_{slot} the channel is

occupied by the message transmission) are random variables identically and independently distributed.¹ The results presented in this paper have been obtained by assuming a geometric distribution for the message length. In [10], similar results have been obtained also with deterministic and bimodal distributions.

3 ENERGY CONSUMPTION AND EFFICIENCY IN p -PERSISTENT CSMA ACCESS SCHEMES

The target for our environment would be both to maximize the network capacity and to minimize the network-interface energy consumption. But how does capacity hamper power saving? It may appear that these two targets cannot be achieved together. Specifically, it seems that to maximize the network capacity the users must be greedy, i.e., transmitting as much as possible. On the other hand, minimization of the network-interface energy seems to indicate that the network should be lightly loaded, i.e., sporadic accesses to the network. In this paper, we will show that, for p -persistent CSMA access schemes, the main performance figures (capacity and energy consumption) are not orthogonal, i.e., the network state that optimizes one index is not far from being optimal also for the other one. To show this result, we analytically study our system, i.e., we derive the relationships that characterize ρ and ρ_{energy} .

As shown in Proposition 2 below, the study of protocol efficiency can be expressed as a special case of the energy consumption analysis. Hence, in the paper, we concentrate on studying the energy consumption only. When necessary, we customize the energy consumption results for analyzing the protocol efficiency. However, before focusing on the energy consumption study, it is useful to introduce a formal definition of the protocol capacity. This is given in Section 3.1. In Section 3.2, we develop an analytical model to study the energy consumption for a p -persistent CSMA access scheme. In Section 3.3, we propose an approximate analysis of the energy consumption to derive a quasi-optimal energy state. Finally, in Section 3.4, we exploit this approximate analysis to derive a closed formula for the p_{opt}^E value that we compare with the closed formula for the p_{opt}^C derived in the same section.

3.1 Protocol Capacity

The channel utilization is the fraction of the channel bandwidth used by successfully transmitted messages. According to the assumptions in our protocol model and considering the p -persistent protocol behavior, we can assess that all the processes that define the channel occupancy pattern (i.e., empty slots, collisions, and successful transmissions) are regenerative with respect to the sequence of time instants corresponding to the completion of a transmission attempt. Hence, the channel utilization can be studied by taking as system regenerative points each completion of a transmission attempt.

1. To simplify the presentation, hereafter, we also assume that consecutive transmission attempts of a station are independent. In the real case, successive retransmissions of the same message obviously have the same length. It is not shown in this paper but (since our results are only based on the average message length) it is possible, even though it is a bit complex, to remove this independent assumption still obtaining the same results presented in the paper.

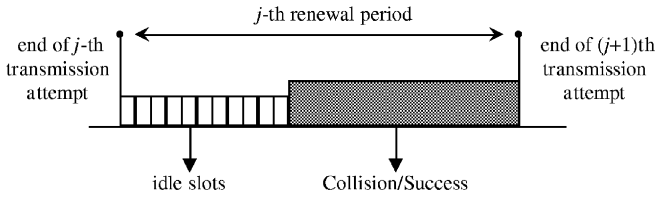


Fig. 1. Structure of the renewal interval.

The structure of the renewal interval is shown in Fig. 1. As shown in the figure, the j th renewal period (i.e., the time between the end of j th and $(j+1)$ th transmission attempt) is made up of a number of consecutive empty slots (idle period) followed by a (successful or colliding) transmission attempt. Hence, the channel utilization ρ is the average time (during a renewal interval) the channel is used to successfully transmit a message, divided by the average length of the renewal interval [23]:

$$\rho = \frac{l \cdot t_{slot} \cdot P_{Succ|N_{tr} \geq 1}}{E[Idle_p] + E[Transmission\ attempt|N_{tr} \geq 1]}, \quad (1)$$

where:

- N_{tr} is the number of stations that begin a transmission in the same slot.
- l is the average message transmission time, normalized to the t_{slot} .
- $P_{Succ|N_{tr} \geq 1}$ is the probability that a transmission attempt is successful.
- $E[Idle_p]$ is the average length of the idle period that precedes a transmission attempt.
- $E[Transmission\ attempt|N_{tr} \geq 1]$ is the average length of a transmission attempt conditioned on the event that at least one transmission occurs.

By indicating with $E[Coll|Collision]$ the average length of a collision given that a collision occurs, we obtain:

$$E[Transmission\ attempt|N_{tr} \geq 1] = l \cdot t_{slot} \cdot P_{Succ|N_{tr} \geq 1} + E[Coll|Collision] \cdot P_{Coll|N_{tr} \geq 1}, \quad (2)$$

where $P_{Coll|N_{tr} \geq 1}$ is the probability to observe a collision given that at least a station is transmitting. By exploiting $E[Idle_p]$, $P_{Succ|N_{tr} \geq 1}$, and $P_{Coll|N_{tr} \geq 1}$ reported in Appendix A (see Lemma A.1), we obtain the analytical formula for the channel utilization ρ :

$$\rho = \frac{l \cdot t_{slot} \cdot M p (1-p)^{M-1}}{(1-p)^M \cdot t_{slot} + l \cdot t_{slot} \cdot M p (1-p)^{M-1} + E[Coll|Collision] \cdot \{1 - [(1-p)^M + M p (1-p)^{M-1}]\}}. \quad (3)$$

As it appears from (3), the channel utilization is a function of the protocol parameter p , and the network configuration, i.e., the number of active stations (M) and the message length distribution. Hence, for a given network configuration, the channel utilization is just a function of p . Therefore, we indicate with p_{opt}^C the p value that maximizes the channel utilization, i.e., the p value associated to the protocol capacity, ρ_{MAX} . Hence, a network achieves its optimal channel utilization if all the stations in the network adopt the p_{opt}^C value as their transmission probability.²

2. Hereafter, we indicate with *optimal capacity state* the network state in which the optimal p value is adopted by each station.

Remark. In a M -station network that adopts a S-ALOHA access scheme, the p_{opt}^C is equal to $1/M$ and the protocol capacity is:

$$\rho_{MAX(Slotted-ALOHA)} = \frac{M}{M-1} \cdot \left(1 - \frac{1}{M}\right)^M. \quad (4)$$

To derive (4), we write the ρ expression for the S-ALOHA access scheme by considering a deterministic message length distribution³ and substituting $l=1$ in (3). By maximizing (3) with classical maximization techniques, we find that $p_{opt}^C = 1/M$ (see also [31]). Hence, the protocol capacity for the S-ALOHA access scheme is simply obtained by substituting $p_{opt}^C = 1/M$ in (3). Equation (4) provides the well-known result for the protocol capacity in an S-ALOHA access scheme [2] and, for an infinite network population, it gives the well-known value $\rho_{MAX(Slotted-ALOHA)} = e^{-1} \approx 0.36788$.

3.2 An Analytical Model for the Energy Consumption

In this section, we develop an analytical model to investigate the energy consumption for p -persistent CSMA access schemes and to derive the network operating point that corresponds to the *optimal energy state*. From an energy consumption standpoint, the network interface alternates between two different phases: the transmitting phase, during which it consumes power to transmit the message to the physical channel, and the receiving phase, during which it consumes power to listen to the physical channel. Hereafter, we denote with PTX and PRX the power consumption (expressed in mW) of the network interface during the transmitting and receiving phase, respectively. The energy drained by the network interface during a time interval will be expressed in millijoule (mJ).

An analytical model for the energy consumption in p -persistent IEEE 802.11 MAC protocol was developed in [8]. In that work, an analytical expression was derived for the energy drained by a tagged-station network-interface to successfully transmit a packet. Specifically, that analysis is based on the observation that the system behavior is regenerative with respect to the time instants corresponding to the successful completion of the tagged-station transmissions. Hence, the energy consumption analysis can be performed by studying the system behavior in the interval between two consecutive regenerative points, henceforth referred to as *virtual transmission time*. Specifically, the system efficiency, from the energy standpoint, is the ratio between the energy used in a renewal interval to successfully transmit a message divided by the average energy consumed by the network interface during a renewal interval:

$$\rho_{energy} = \frac{PTX \cdot l \cdot t_{slot}}{E[Energy_{virtual_transmission_time}]}, \quad (5)$$

where $E[Energy_{virtual_transmission_time}]$ is the energy consumed by the tagged station in a virtual transmission time, and l is the average message transmission time normalized to the t_{slot} .

Hereafter, we will denote with $E[Energy_{xxx}|YY]$ the average energy consumed by a station in a type xxx interval

3. For a deterministic message length distribution $E[Coll|Collision]$ is equal to l .

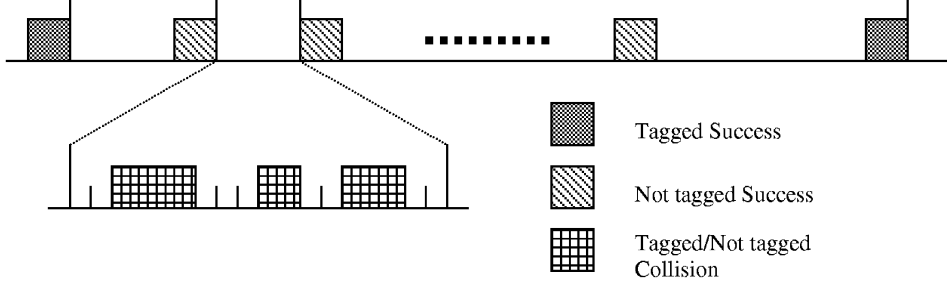


Fig. 2. Channel structure during a virtual transmission time.

(for instance, during an idle period, a transmission attempt, a tagged station success, etc.) conditioned on the occurring of event YY (for instance, a tagged-station transmission, a not tagged station transmission, etc.).

As shown in Fig. 2, the virtual transmission time can be partitioned into: idle periods, collisions, and successful transmissions. Collisions and successful transmissions can be further partitioned into two subsets depending on if the tagged station is involved. This distinction is useful because the impact of the PTX parameter is different during tagged and not-tagged collisions.

The analytical formulas derived in [8] are complex and not suitable for runtime tuning of a network. For this reason, in this paper, we re-elaborate that analysis to achieve a simpler characterization of the energy consumption. With this simplified characterization:

1. We define the exact formula for the numerical computation of the optimal p value from the energy consumption standpoint, p_{opt}^E .
2. We provide and validate a heuristic formula for an energy-efficient tuning of the network.
3. We derive and validate a closed formula for p_{opt}^E .

Let us now start to re-elaborate the energy consumption analysis. Our analysis is based on the observation that the system behavior is regenerative also with respect to the time instants corresponding to the completion of each transmission attempt (i.e., successful transmission or collision). Hence, the $E[Energy_{virtual_transmission_time}]$ can be expressed also as:

$$E[Energy_{virtual_transmission_time}] = E[N_{ta}] \cdot E[Energy_{transmission_attempt_interval}],$$

where $E[Energy_{transmission_attempt_interval}]$ is the energy consumed by the tagged station between two consecutive transmission attempts and $E[N_{ta}]$ is the average number of transmission attempts in the same time interval.

It is also worth noting that $1/E[N_{ta}]$ is the probability that a transmission attempt is a successful transmission of the tagged station (given that a transmission attempt occurs). Hereafter, this probability is denoted as $P_{tag_Succ|N_{tr} \geq 1}$, i.e., $P_{tag_Succ|N_{tr} \geq 1} = 1/E[N_{ta}]$.

Hence, (5) can be rewritten as:

$$\rho_{energy} = \frac{PTX \cdot l \cdot t_{slot} \cdot P_{tag_Succ|N_{tr} \geq 1}}{E[Energy_{Idle_p}] + E[Energy_{transmission_attempt|N_{tr} \geq 1}]}, \quad (6)$$

where:

- N_{tr} is the number of stations that begin to transmit at the same slot.
- l is the average message transmission time, normalized to the t_{slot} .
- $P_{tag_Succ|N_{tr} \geq 1}$ is the probability of a tagged-station successful transmission given that there is a transmission attempt.
- $E[Energy_{Idle_p}]$ is the average energy consumed by the tagged station during the idle period that precedes a transmission attempt.
- $E[Energy_{transmission_attempt|N_{tr} \geq 1}]$ is the average energy consumed during a transmission attempt given that at least one station is transmitting.

Formula (6) indicates that the energy efficiency can also be expressed as the ratio between the average energy used by the tagged station in a transmission attempt interval to successfully transmit a message divided by the total energy consumed by the tagged-station network-interface during a transmission attempt interval.

The unknown quantities in (6) are given by the following Lemma.

Lemma 1. *In a M -station network that adopts a p -persistent CSMA access scheme, by assuming that each station is operating in asymptotic conditions and the sequence of message lengths $\{L_i\}$, normalized to t_{slot} , are i.i.d. geometrically distributed (with parameter q) random variables:*

$$E[Energy_{Idle_p}] = PRX \cdot E[Idle_p] = PRX \cdot t_{slot} \frac{(1-p)^M}{1-(1-p)^M}, \quad (7.a)$$

$$P_{tag_Succ|N_{tr} \geq 1} = \frac{p(1-p)^{M-1}}{1-(1-p)^M}, \quad (7.b)$$

$$P_{not_tag_Succ|N_{tr} \geq 1} = \frac{(M-1)p(1-p)^{M-1}}{1-(1-p)^M},$$

$$E[Energy_{transmission_attempt|N_{tr} \geq 1}] = E[Energy_{tag_Succ|tag_Succ}] \cdot P_{tag_Succ|N_{tr} \geq 1} + E[Energy_{not_tag_Succ|not_tag_Succ}] \cdot P_{not_tag_Succ|N_{tr} \geq 1} + E[Energy_{tag_Coll|tag_Coll}] \cdot P_{tag_Coll|N_{tr} \geq 1} + E[Energy_{not_tag_Coll|not_tag_Coll}] \cdot P_{not_tag_Coll|N_{tr} \geq 1}, \quad (7.c)$$

where:

$$\begin{aligned} E[Energy_{tag_Succ}|tag_Succ] &= PTX \cdot l \cdot t_{slot}, \\ E[Energy_{not_tag_Succ}|not_tag_Succ] &= PRX \cdot l \cdot t_{slot}, \end{aligned} \quad (8.a)$$

$$\begin{aligned} E[Energy_{tag_Coll}|tag_Coll] &= PTX \cdot t_{slot} \cdot (1/(1-q)) + PRX \\ &\cdot \frac{t_{slot}}{1 - (1-p)^{M-1}} \cdot \sum_{x=1}^{\infty} q^{x-1} (1-q) \\ &\cdot \left[\sum_{y=1}^{\infty} y \cdot \left[(1-pq^{y+x})^{M-1} \right. \right. \\ &\left. \left. - \left(1 - pq^{y+x-1} \right)^{M-1} \right] \right], \end{aligned} \quad (8.b)$$

$$P_{tag_Coll|N_{tr} \geq 1} = \frac{p \cdot (1 - (1-p)^{M-1})}{1 - (1-p)^M}, \quad (8.c)$$

$$\begin{aligned} P_{not_tag_Coll|N_{tr} \geq 1} &= \\ \frac{(1-p) \left(1 - (1-p)^{M-1} - (M-1) \cdot p \cdot (1-p)^{M-2} \right)}{1 - (1-p)^M}, \end{aligned} \quad (8.d)$$

$$\begin{aligned} E[Energy_{not_tag_Coll}|not_tag_Coll] &= \\ PRX \cdot E[Coll_{not_tag}|not_tag_Coll] &= \\ \frac{t_{slot}}{1 - \left[(1-p)^{M-1} + (M-1)p(1-p)^{M-2} \right]} \cdot \\ \left[\sum_{h=1}^{\infty} \left\{ h \cdot \left[(1-pq^h)^{M-1} - (1-pq^{h-1})^{M-1} \right] \right\} \right. \\ \left. - \frac{(M-1)p(1-p)^{M-2}}{1-q} \right]. \end{aligned} \quad (8.e)$$

Proof. The derivation of the above formulas is based on classical probabilistic arguments. Formula (7.a) immediately follows from Lemma A.1 results (see Appendix A). Formulas (7.b), (8.c), and (8.d) can be easily derived by exploiting the definition of conditional probability. Formulas (7.c) and (8.a) are easily derived by exploiting the definition of conditional expectation of event X given event Y . The complete proof of (8.b) can be found in [8]. To obtain (8.e) is enough to notice that $E[Coll_{not_tag}|not_tag_Coll]$ is derived by applying the formula for $E[Coll|Collision]$ assuming a network population of $(M-1)$ stations. \square

At it appears from (6) and Lemma 1, ρ_{energy} is a function of (p, q, M, PTX, PRX) . Hereafter, we refer to p_{opt}^E as the p value that maximizes the energy efficiency ρ_{energy} for a given set of parameters M, q, PTX , and PRX . Hence, a network is in its *optimal energy state* if each station adopts the p_{opt}^E value as its transmission probability. The p_{opt}^E values for several settings of the proposed parameters can be computed by numerically maximizing (6). Before proceeding with our analysis, we introduce some useful results.

Proposition 1. *In a M -station network that adopts a p -persistent CSMA access scheme, if the stations operate in asymptotic conditions, the average number of successful transmissions in a virtual transmission time is equal to M . Furthermore, the average number of successful transmissions in a virtual transmission time is independent from the p .*

Proof. A p -persistent CSMA access scheme is fair, i.e., all stations have the same throughput. As a virtual transmission time is a renewal period of the system, it follows that the average number of successful transmission is the same for all stations. As the tagged station transmits exactly a packet in each virtual transmission time, it follows that each other station will transmit, in average, one packet per virtual transmission time. \square

Proposition 1 is useful as it indicates that the average energy consumption due to successful transmissions in a virtual transmission time is constant with respect to the p value and, thus, it can be neglected while trying to minimize the tagged station energy consumption. In addition, by exploiting Proposition 1, we can prove the following result that defines the relationship between the capacity and the energy efficiency of a MAC protocol.

Proposition 2. *In an M -station network that adopts a p -persistent CSMA access scheme, if the stations operate in asymptotic conditions and $PTX = PRX$*

$$\rho_{energy} = \frac{\rho}{M}$$

and, hence, $p_{opt}^E = p_{opt}^C$.

Proof. First, let us note that (see Proposition 1)

$$P_{tag_Succ|N_{tr} \geq 1} = P_{Succ|N_{tr} \geq 1} / M.$$

Furthermore, if $PTX = PRX$, then

$$\begin{aligned} E[Energy_{Idle.p}] + E[Energy_{transmission_attempt}|N_{tr} \geq 1] &= \\ PRX \cdot (E[Idle.p] + E[Transmission_attempt|N_{tr} \geq 1]). \end{aligned}$$

Hence, by comparing (1) with (6), it results in $\rho_{energy} = \rho/M$. Thus, the same p value optimizes both indices. \square

Before concluding this section, it is useful to introduce another index to characterize the system from the energy standpoint: the *Energy Consumption*. The Energy Consumption is defined as the average energy (in mJ) consumed by the tagged-station network-interface to successfully transmit a message.

Proposition 3. *In a M -station network that adopts a p -persistent CSMA access scheme, if the stations operate in asymptotic conditions, the Energy Consumption is*

$$Energy\ Consumption = \frac{PTX \cdot l \cdot t_{slot}}{\rho_{energy}}.$$

Proof. The proof is obtained by exploiting the regenerative property of the system and noting that $P_{tag_Succ|N_{tr} \geq 1}$ can be expressed as the ratio between the number of tagged-station successful transmissions in a virtual transmission time and $E[N_{ta}]$, i.e., the average number of transmission attempts in the same time interval. Hence, $P_{tag_Succ|N_{tr} \geq 1} = 1/E[N_{ta}]$ and

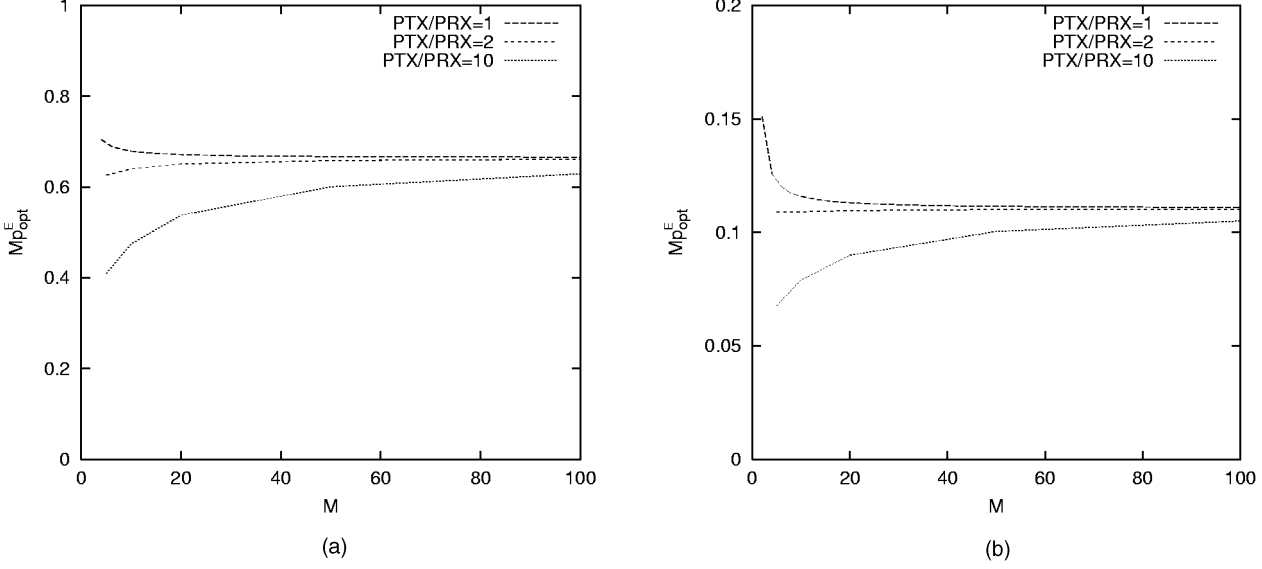


Fig. 3. The $M \cdot p_{opt}^E$ product. (a) $l = 2t_{slot}$. (b) $l = 100t_{slot}$.

$$\rho_{energy} = \frac{PTX \cdot l \cdot t_{slot}}{E[N_{ta}] \left(E[Energy_{idle-p}] + E[Energy_{transmission_attempt|N_{tr} \geq 1}] \right)} \quad (9)$$

The proof immediately follows by noting that the denominator of (9) is the Energy Consumption. \square

In the following, we will show that the optimal network state can be characterized by an invariant figure: the average number of stations that transmit in a slot. Specifically, we will show that this figure can also be adopted to characterize both the “optimal energy state” and the “optimal capacity state.” To this end, let us now focus on the average number of stations that should transmit in a slot to achieve the minimum Energy Consumption, i.e., $M \cdot p_{opt}^E$. Figs. 3a and 3b show the $M \cdot p_{opt}^E$ value for an average message length l equal to either two or 100 time slots, respectively. In each figure, we plot the $M \cdot p_{opt}^E$ value related to different PTX/PRX values. The curves labeled with $PTX/PRX = 1$ correspond also to the $M \cdot p_{opt}^C$ product (see Proposition 2).

From the plotted curves, we observe that the $M \cdot p_{opt}^E$ product exhibits a dependency on the value for small network-size population. This effect is more marked when $PTX/PRX = 10$, while for $PTX/PRX \leq 2$, the $M \cdot p_{opt}^E$ product is almost independent of the M value. In this latter case, the optimal energy state is very close to the optimal capacity state, due to the small difference between $M \cdot p_{opt}^E$ and $M \cdot p_{opt}^C$. In other words, by adopting the p_{opt}^E value as transmission probability, we obtain not only the optimal power saving, but also a quasi-optimal channel utilization. For $PTX/PRX = 10$, the $M \cdot p_{opt}^E$ product shows a significant dependency on the M value. This dependency reduces only for large M value (e.g., $M \geq 50$). This behavior can be explained by observing that the PTX value affects the energy consumed only during tagged-station transmissions and the probability of this event decreases as $1/M$.

3.3 Energy Consumption: An Approximate Analysis

It is desirable to have a simpler relationship than (6) to provide an approximation for the p_{opt}^E value. How this can be achieved is presented in this section. To achieve a simple

approximation of the p_{opt}^E value, in the following, we investigate the role of the various terms of (6) in determining the Energy Consumption. Specifically, in the energy consumption formula, we separate the terms that are increasing functions of the p value from the terms that are decreasing functions of the p value. To achieve this, it is useful to introduce the following proposition.

Proposition 4. *In an M -station network that adopts a p -persistent CSMA access scheme, if the stations operate in asymptotic conditions, ρ_{energy} is equal to*

$$\rho_{energy} = \frac{PTX \cdot l \cdot t_{slot}}{E[N_{ta}] \left(E[Energy_{idle-p}] + PTX \cdot l \cdot t_{slot} + PRX \cdot (M-1) \cdot l \cdot t_{slot} + (E[N_{ta}] - M) \cdot E[Energy_{Coll|N_{tr} \geq 1}] \right)} \quad (10)$$

Proof. The proof requires some algebraic manipulations of (9). According to Proposition 1, the number of successful transmissions in a virtual transmission time is M . Furthermore, in the virtual transmission time, there is exactly one successful transmission of the tagged station and, in average, there are $(M-1)$ successful transmissions of the other stations. From Proposition 1, it is also straightforward to derive that the average number of collisions that we observe within a virtual transmission time is constituted by the total number of transmission attempts in a virtual transmission time less the average number of successful transmissions, i.e., $(E[N_{ta}] - M)$. According to these assessments and by exploiting formula (8.a), (10) immediately follows. \square

From Proposition 4, it follows that p_{opt}^E corresponds to the p value that minimizes the denominator of (10). It is also worth noting that the second and third term of this denominator do not depend on the p value and, hence, they play no role in the minimization process. Now, our problem reduces to find

$$\min_p \left\{ E[N_{ta}] \cdot E[Energy_{idle-p}] + (E[N_{ta}] - M) \cdot E[Energy_{Coll|N_{tr} \geq 1}] \right\} \quad (11)$$

TABLE 1
Capacity Analysis with a Geometric Message-Length Distribution ($PTX/PRX = 1$)

l (t_{slot})	Optimal ρ			Quasi-Optimal ρ		
	$M=10$	$M=50$	$M=100$	$M=10$	$M=50$	$M=100$
	2	0.446598	0.431628	0.429849	0.445040	0.429569
5	0.561334	0.547862	0.546249	0.560622	0.546912	0.545268
10	0.646985	0.635186	0.633766	0.646622	0.634698	0.633263
20	0.724072	0.714196	0.713004	0.723897	0.713962	0.712761
50	0.807864	0.800508	0.799617	0.807801	0.800424	0.799530
100	0.857003	0.851324	0.850634	0.856974	0.851285	0.850594

Now, let us note that the first term in (11), i.e., $E[N_{ta}] \cdot E[Energy_{Idle-p}]$, after some algebraic manipulations reduces to $[PRX \cdot t_{slot} \cdot (1-p)]/p$ and, thus, this first term is a decreasing function of p . On the other hand, the second term in (11) is an increasing function of p . Following the same line of reasoning adopted in [19] to optimize a CSMA protocol (see also [12]), we propose to approximate the p_{opt}^E value with the p value that balances the increasing and decreasing costs of p :

$$E[N_{ta}] \cdot E[Energy_{Idle-p}] = (E[N_{ta}] - M) \cdot E[Energy_{Coll}|N_{tr} \geq 1]. \quad (12)$$

Equation (12) means that energy consumed during idle periods should be equal to the energy consumed during collisions to obtain a quasioptimal (i.e., minimal) Energy Consumption. Equation (12) can be rewritten as:

$$E[Energy_{Idle-p}] = E[Energy_{Coll}|N_{tr} \geq 1] \cdot P_{Coll|N_{tr} \geq 1}. \quad (13)$$

To ease the computation of $E[Energy_{Coll}|N_{tr} \geq 1]$, we subdivide the collisions in two subsets depending on whether or not they involve the tagged station. Specifically, by exploiting formulas (7.c), (8.c), and (8.d), (13) can be rewritten as:

$$E[Energy_{Idle-p}] = E[Energy_{tag-Coll}|tag-Coll] \cdot P_{tag-Coll|N_{tr} \geq 1} + E[Energy_{not_tag-Coll}|not_tag-Coll] \cdot P_{not_tag-Coll|N_{tr} \geq 1}. \quad (14)$$

Equation (14) defines a simple but approximate relationship to characterize p_{opt}^E . Before using it, it is necessary to investigate its accuracy. In Table 1, we compare the maximum efficiency, calculated by maximizing (3), and the quasi-optimal efficiency measured when each station adopts the p value that solves (14) with $PTX/PRX = 1$, say p_{HE}^C . At the same way, in Tables 2 and 3, we compare the minimum Energy Consumption, calculated by minimizing (6) and the quasi-optimal Energy Consumption measured when each station adopts the p value that solves (14) with $PTX/PRX > 1$, say p_{HE}^E . To avoid useless details, we assume that our power unit is the power consumption when the network is in the receiving state, i.e., $PRX = 1$. The numerical results are obtained by assuming $PTX = 2$ or $PTX = 10$ [24].

The results listed in the tables seem to indicate that the heuristic approximation, provided by (14), is amazingly precise: The approximations show an error always lower than 1 percent of the exact values. This precision, as will

TABLE 2
Energy Consumption Analysis with a Geometric Message-Length Distribution ($PTX/PRX = 2$)

l (t_{slot})	Energy Consumption					
	Optimal Value			Quasi-Optimal Value		
	$M=10$	$M=50$	$M=100$	$M=10$	$M=50$	$M=100$
2	48.47725	235.5270	469.1458	48.6354	236.6402	471.4583
5	96.58502	464.0322	923.0718	96.6980	464.8253	924.7191
10	168.0429	800.9190	1591.650	168.1293	801.5233	1592.904
20	301.0818	1425.404	2830.308	301.1478	1425.864	2831.263
50	676.5500	3181.204	6311.251	676.5972	3181.531	6311.929
100	1277.622	5984.743	11867.66	1277.661	5985.009	11868.11

TABLE 3
Energy Consumption Analysis with a Geometric Message-Length Distribution ($PTX/PRX = 10$)

l (t_{slot})	Energy Consumption					
	Optimal Value			Quasi-Optimal Value		
	$M=10$	$M=50$	$M=100$	$M=10$	$M=50$	$M=100$
2	74.96422	265.2548	499.5055	75.11057	266.3723	501.8313
5	152.5067	524.3949	984.2585	152.6086	525.1826	985.9046
10	270.2620	909.1103	1700.930	270.3388	909.7076	1702.181
20	492.2676	1624.782	1624.782	492.3255	1625.235	3032.113
50	1125.580	3642.874	6775.180	1125.620	3643.194	6776.852
100	2146.786	6871.577	12757.54	2146.819	6871.836	12758.09

show below, is not due only to the accuracy of the p_{HE}^C and p_{HE}^E , but is also caused by the low sensitiveness of both ρ and ρ_{energy} to the p value.

Fig. 4 shows the relative error⁴ between the p value that maximizes (3), i.e., p_{opt}^C and p_{HE}^C , versus the average message length. Fig. 4 also shows the relative error between the exact protocol capacity and the quasi-optimal one. Note that the relative error related to the ρ approximation is always a magnitude lower than the relative error related to the p_{opt}^C approximation. Furthermore, the distance between the relative errors related to p_{opt}^C and ρ approximations decreases rapidly when the message-length increases. In conclusion, we can assess that the protocol capacity has a low sensitiveness to a deviation of the p value from the p_{opt}^C . For example, in our results a 10 percent deviation from the p_{opt}^C causes an error on the ρ value always less than 1 percent. In addition, for average message lengths greater than 10 slots, the error on the ρ value is always less than 0.1 percent.

Figs. 5a and 5b show (for several message lengths) the relative error between p_{opt}^E and p_{HE}^E for $PTX/PRX = 2$ and $PTX/PRX = 10$, respectively. Figs. 5a and 5b also show the relative error between the minimum Energy Consumption and its approximate value obtained from (14). The observations we have drawn for the capacity (see Fig. 4) hold also for the Energy Consumption case. Hence, we can assess that the energy consumption has a low sensitiveness to a deviation of the p value from the p_{opt}^E , and the errors introduced by our approximation are always very low.

4. The relative error is defined as the difference between the exact value and the approximate value normalized to the exact value.

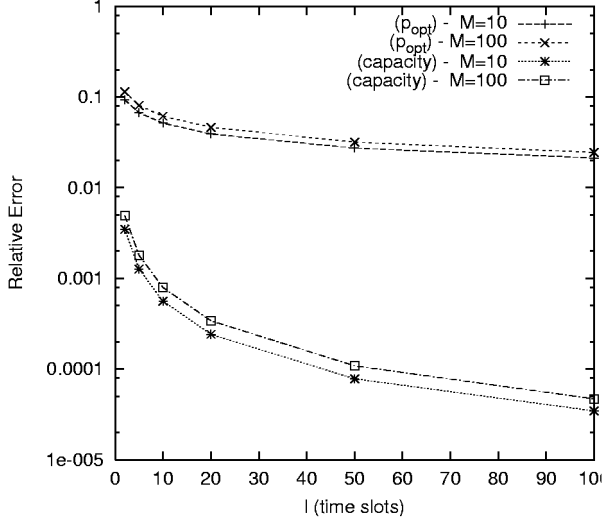


Fig. 4. Relative errors related to p_{opt}^C and ρ_{max} approximations.

From the discussion performed so far, it results that the Energy Consumption minimization can be achieved not only by the complex numerical computation of the p value that minimizes (6), but it is sufficient to identify the p value that permits having $E[Energy_{Idle-p}]$ equal to $E[Energy_{Coll}|N_{tr}=1]$.

It is straightforward to notice that many similarities exist between the channel-utilization maximization issue and the Energy Consumption minimization issue. In the following, we investigate in depth the relationship between the optimal capacity state and the optimal energy state.

Figs. 3a and 3b provide a preliminary comparison between p_{opt}^C and p_{opt}^E . Let us remind that the p_{opt}^C corresponds to the curve with $PTX = PRX$. These figures show that: 1) the p_{opt}^E values are always lower than the p_{opt}^C values, and 2) the differences tend to disappear by increasing M . Hereafter, we will better analyze the relationship between p_{opt}^C and p_{opt}^E by focusing on a small network ($M = 10$) for which, as shown in Figs. 3a and 3b, the differences are meaningful. Specifically, in Fig. 6, we have plotted $E[Energy_{Idle-p}]$ and $E[Energy_{Coll}|N_{tr} \geq 1]$ versus the p value, for various PTX/PRX values. $E[Energy_{Idle-p}]$ is equal to $E[Idle-p]$ due to the assumption that $PRX = 1$ (see (17.a)). The p value that corresponds to the intersection point of the $E[Energy_{Idle-p}]$ and $E[Energy_{Coll}|N_{tr} \geq 1]$ curves is the approximation of the p_{opt}^E value, as (14) indicates. As the $E[Energy_{Coll}|N_{tr} \geq 1]$ related to $PTX/PRX = 1$ is equal to the average length of a collision given a transmission attempt, i.e., $E[Coll|N_{tr} \geq 1]$, the p value that corresponds to the intersection point of the $E[Idle-p]$ and $E[Coll|N_{tr} \geq 1]$ curves provides a good approximation of the p_{opt}^C value, as (14) indicates. We note that, by increasing the PTX value also $E[Energy_{Coll}|N_{tr} \geq 1]$ grows due to the rise in the energy consumption of tagged-station collisions. However, $E[Energy_{Idle-p}]$ does not depend on the PTX value, hence, only a decrease in the p_{opt}^E value can balance the increase in $E[Energy_{Coll}|N_{tr} \geq 1]$.

3.4 Energy Consumption: A p_{opt}^E Closed Formula

We conclude the characterization of our system, from the Energy Consumption standpoint, by providing closed (approximate) formulas to identify the network state that minimizes the Energy Consumption.

The closed formulas are derived with the assumption that collisions involve exactly two stations:⁵

$$E[Energy_{not_tag_Coll}|not_tag_Coll] \approx E[Energy_{not_tag_Coll}|not_tag_Coll, N_{tr} = 2] = \bar{E}_{CNT}, \quad (15.a)$$

$$E[Energy_{tag_Coll}|tag_Coll] \approx E[Energy_{tag_Coll}|tag_Coll, N_{tr} = 2] = \bar{E}_{CT}, \quad (15.b)$$

where the \bar{E}_{CNT} and \bar{E}_{CT} formulas are derived in Appendix B.

By assuming a geometric message-length distribution (with parameter q), the above formulas become (see Appendix B):

$$E[Energy_{not_tag_Coll}|not_tag_Coll] \approx PRX \cdot \frac{1+2q}{(1-q)(1+q)} = PRX \cdot \bar{C} = \bar{E}_{CNT}, \quad (16.a)$$

$$E[Energy_{tag_Coll}] \approx \frac{1}{1-q} \cdot \left[PTX + PRX \cdot \frac{q}{1+q} \right] = \bar{E}_{CT}. \quad (16.b)$$

In Tables 4 and 5, by assuming that all the stations adopt the p_{opt}^E value as their transmission probability, we compare the exact values of the average energy consumed during tagged-station collisions (see (8.b)) and during not tagged-station collisions (see (8.e)) with the approximations provided by (16.a) and (16.b), respectively. In the tables, we analyze the cases $PTX/PRX = 2$ and $PTX/PRX = 10$. Similar results have been obtained also for $PTX/PRX = 1$.

The numerical results reported in the tables confirm that both expressions (15.a) and (15.b) provide precise approximations of $E[Energy_{tag_Coll}|tag_Coll]$ and

$$E[Energy_{not_tag_Coll}|not_tag_Coll].$$

Furthermore, the numerical results show that both $E[Energy_{tag_Coll}|tag_Coll]$ and

$$E[Energy_{not_tag_Coll}|not_tag_Coll]$$

do not significantly depend on the M value, while they depend on the average message length and the PTX and PRX values.

By exploiting the above approximations on the energy consumption during a collision (see (15.a) and (15.b)), we are now able to prove the following lemma that provides a closed formula for p_{opt}^E and p_{opt}^C .

Lemma 2. In an M -station network in which the message lengths $\{L_i\}$, normalized to t_{slot} , are a sequence of i.i.d. random variables, under the condition $Mp \ll 1$ the p_{opt}^E value is

$$p_{opt}^E \cong \frac{\sqrt{1 + 2 \frac{M-1}{M} \left[\bar{C} \cdot \frac{(M-2)}{M} + \frac{\bar{E}_{CT}}{PRX} \cdot \frac{1}{M} - 1 \right]} - 1}{(M-1) \left[\bar{C} \cdot \frac{(M-2)}{M} + \frac{\bar{E}_{CT}}{PRX} \cdot \frac{1}{M} - 1 \right]}, \quad (17)$$

where $\bar{C} = E[\max\{L_1, L_2\}]$ and

$$\bar{E}_{CT} = E[Energy_{tag_Coll}|tag_Coll, N_{tr} = 2].$$

5. We propose this approximation as previous work [12] has shown that 1) the collision probability is low when the network is close to its optimal capacity state, and 2) given a collision, the probability that more than two stations collide is negligible.

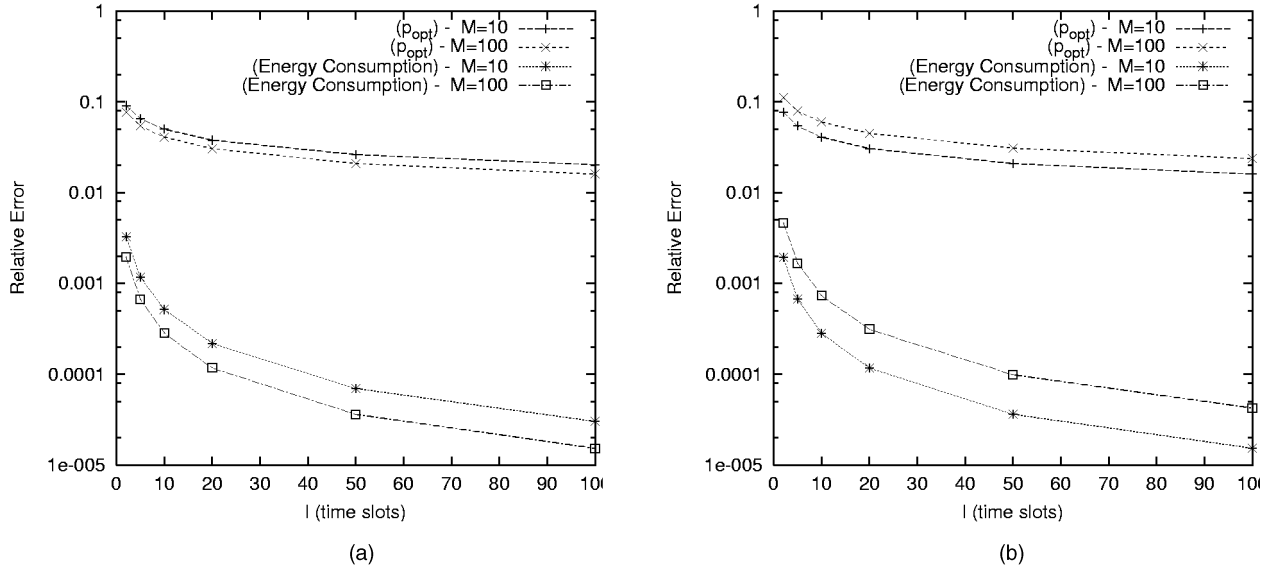


Fig. 5. Relative errors related to p_{opt}^E and the minimum Energy consumption approximations. (a) $PTX/PRX = 2$. (b) $PTX = PRX = 10$.

Proof. We assume that p_{opt}^E is identified by (14). The proof is based on (15.a) and (15.b). Specifically, (14) can be rewritten as:

$$PRX \cdot (1-p)^M = PRX \cdot \bar{C} \cdot p \left[1 - (1-p)^{M-1} \right] + \bar{E}_{CNT} \cdot (1-p) \left\{ 1 - \left[(1-p)^{M-1} + (M-1)p(1-p)^{M-2} \right] \right\}. \quad (18)$$

Furthermore, under the condition $Mp \ll 1$, we have:

$$(1-p)^M = 1 - Mp + \frac{M(M-1)}{2} p^2 - O((Mp)^3) \xrightarrow{Mp \ll 1} 1 - Mp + \frac{M(M-1)}{2} p^2, \quad (19.a)$$

$$p \left[1 - (1-p)^{M-1} \right] = \frac{(M-1)}{2} p^2 + O((Mp)^3) \xrightarrow{Mp \ll 1} \frac{(M-1)}{2} p^2, \quad (19.b)$$

$$(1-p) \left\{ 1 - \left[(1-p)^{M-1} + (M-1)p(1-p)^{M-2} \right] \right\} = \frac{(M-1)(M-2)}{2} p^2 + O((Mp)^3) \xrightarrow{Mp \ll 1} \frac{(M-1)(M-2)}{2} p^2. \quad (19.c)$$

These approximations yield to the following approximate expression of (14):

$$1 - Mp + \frac{M(M-1)}{2} p^2 = \bar{C} \cdot \frac{(M-1)(M-2)}{2} p^2 + \frac{\bar{E}_{CNT}}{PRX} \cdot \frac{(M-1)}{2} p^2. \quad (20)$$

Formula (17) is obtained by solving (20). This concludes the proof. \square

Proposition 5. In an M -station network in which the message lengths $\{L_i\}$, normalized to t_{slot} , are a sequence of i.i.d. random variables, under the condition $Mp \ll 1$ the p_{opt}^C value is

$$p_{opt}^C \cong \frac{\sqrt{1 + 2 \frac{M-1}{M} \left[\bar{C} \cdot \frac{(M-1)}{M} - 1 \right]} - 1}{(M-1) \left[\bar{C} \cdot \frac{(M-1)}{M} - 1 \right]} \quad (21)$$

$$\xrightarrow{M \gg 1} \frac{1}{M} \cdot \frac{\sqrt{1 + 2(\bar{C} - 1)} - 1}{(\bar{C} - 1)} \xrightarrow{\bar{C} \gg 1} \frac{1}{M \cdot \sqrt{2\bar{C}}},$$

where $\bar{C} = E[\max\{L_1, L_2\}]$.

Proof. The first part of (21) immediately follows from (17) when $PTX = PRX = 1$. The other derivations are simple algebraic manipulations. \square

It is worth pointing out that (21) has been obtained and validated also in [5] for the IEEE 802.11 WLAN in the case of a deterministic message length.

The following proposition provides an analytical investigation of the $M \cdot p_{opt}^E$ for a large network-size population.

Proposition 6. In an network with a large number of active stations ($M \gg 1$) in which the message lengths $\{L_i\}$,

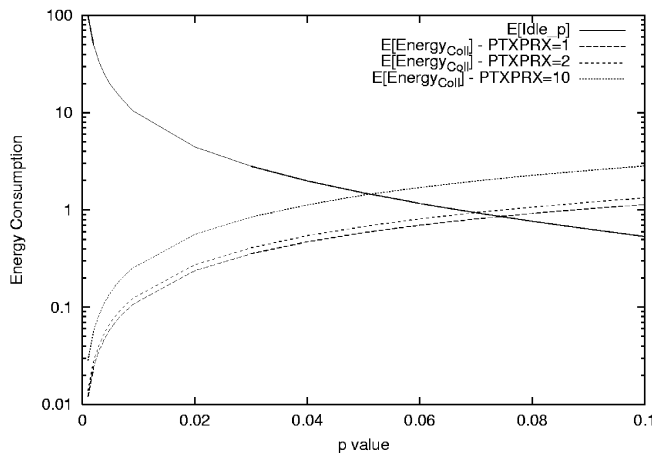


Fig. 6. p_{opt}^E approximation with $M = 10$ and $l = 2t_{slot}$.

TABLE 4
 $E[Energy_{tag_Coll}|tag_Coll]$

$l (t_{slot})$	$PTX/PRX = 2$			$PTX/PRX = 10$		
	Exact Value		Approximate Value	Exact Value		Approximate Value
	$M=10$	$M=100$		$M=10$	$M=100$	
2	4.79701852	4.82917589	4.6666667	20.76174773	20.82097446	20.6666667
10	25.1497834	25.2478778	24.7368421	105.0380555	105.2235770	104.7364842
100	251.188393	251.532828	249.748743	1052.896228	1051.445834	1049.748744

TABLE 5
 $E[Energy_{not_tag_Coll}|not_tag_Coll]$

$l (t_{slot})$	Exact Value ($PTX/PRX = 2$)		Exact Value ($PTX/PRX = 10$)		Approximate Value
	$M=10$	$M=100$	$M=10$	$M=100$	
	2	2.7438022744	2.7756241919	2.7225317652	
10	14.9537384520	15.0550105599	14.8794813950	15.0378314137	14.73684211
100	149.4496056877	149.9934805697	151.037447459	149.891435366	149.7487437

normalized to t_{slot} , are a sequence of i.i.d. random variables, the optimal $M \cdot p_{opt}^E$ value is:

$$M \cdot p_{opt}^E \xrightarrow{M \gg 1} \frac{\sqrt{1 + 2(\bar{C} - 1)} - 1}{(\bar{C} - 1)} \xrightarrow{\bar{C} \gg 1} \frac{1}{\sqrt{2\bar{C}}} \quad (22)$$

Proof. The proof of this proposition is straightforward. Under the condition $M \gg 1$, (17) can be rewritten as (21) by noting that $(M - 1) \approx M$ and $(M - 2) \approx M$. \square

As the right-hand side of (22) does not depend on the PTX and PRX values, the obtained result directly applies also to $M \cdot p_{opt}^C$. This investigation is useful because it shows how for a large network size population the p_{opt}^E value tends to the p_{opt}^C value. Through Propositions 5 and 6, we have provided a formal proof of the tight analogy between the $M \cdot p_{opt}^C$ and the $M \cdot p_{opt}^E$ values, analogy that we have numerically validated in the previous section in the Figs. 3a and 3b.

To validate our approximated formulas for $M \cdot p_{opt}^C$ and $M \cdot p_{opt}^E$, in Fig. 7, we compare the $M \cdot p_{opt}^C$ and $M \cdot p_{opt}^E$ approximate values (evaluated through (22)) with the exact values obtained by the numerical solution of (3) and (10), respectively. Specifically, in the figure, we report the $M \cdot p_{opt}$ value for several PTX/PRX ratios and by considering both short and long messages. The results obtained indicate that the accuracy of the approximation increases with the increase of the message length and the number of the active stations. Furthermore, as expected, for $PTX/PRX \leq 2$, the approximations are very accurate starting from $M > 5$. On the other hand, for $PTX/PRX = 10$, the impact of the tagged station transmission on the energy consumption is large (as it costs PTX per time unit) and this explains the error introduced by approximation (22) that neglects this cost. Obviously, as the probability of a tagged transmission during a virtual transmission time is equal to $1/M$, the accuracy of the approximation increases by increasing the

M value. As far as the protocol capacity, the figure shows that in all the configurations analyzed, the approximate $M \cdot p_{opt}^C$ value is very close to the exact numerical value.

4 TRANSMISSION CONTROL STRATEGIES TO ATTAIN POWER-SAVING/EFFICIENCY OPTIMIZATION

In Sections 2 and 3, we have developed the mathematical framework required to study both the channel utilization and Energy Consumption performances in the p -persistent CSMA access scheme. From these investigations, we derived the network operating points corresponding to a quasi-optimal capacity state and to a quasi-optimal energy state. In the following, the results previously obtained will be exploited to define a transmission control strategy to attain power saving optimization. Due to the tight analogies

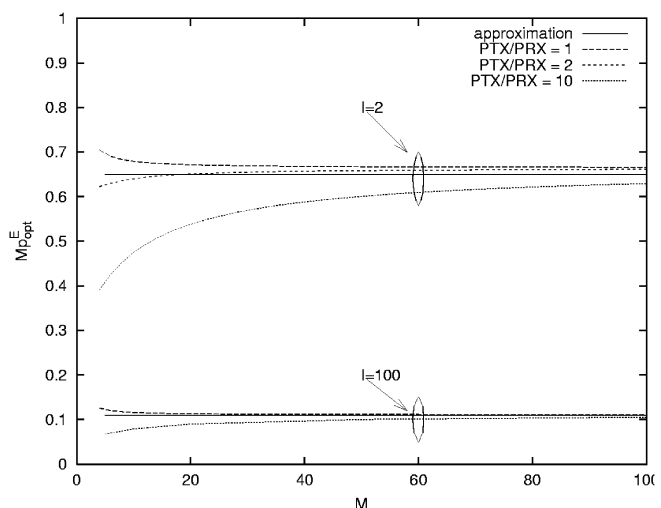


Fig. 7. Accuracy of $M \cdot p_{opt}^C$ and $M \cdot p_{opt}^E$ approximate formulas.

between efficiency and power saving in *p*-persistent CSMA access scheme, the transmission control strategy to attain the protocol capacity is simply a special case of the power saving strategy.

4.1 The State of the Art in Feedback-Based Multiaccess Protocols

Before introducing the transmission control strategies for channel utilization maximization and Energy Consumption minimization, we review the literature on feedback-based multiaccess protocols. This review has a twofold objective. One objective is to present the key results obtained in the last decades to stabilize the performance of random access protocols (mainly, ALOHA and CSMA access schemes). The other objective is to better highlight the relationship between our approach and previous proposals. As we have shown in previous sections, both p_{opt}^E and p_{opt}^C depend on the network and traffic conditions. Hence, the protocol capacity and the minimum Energy Consumption can only be achieved if the value is dynamically tuned at runtime following the evolution of the network and traffic conditions. To perform this tuning, a station must have an exact knowledge of the network status. Unfortunately, in a real case, a station does not have an exact knowledge of the network configuration (the number of active stations belonging to the network) and traffic characteristics (length of the messages transmitted on the channel), but it can, at most, estimate it by observing the channel status.

The idea to use a feedback from the channel status to tune at runtime the backoff algorithm in a random access protocol is not new and many strategies have been proposed in literature [21], [25], [20]. Rivest proposed a *ternary feedback* model by which the three events that each station needs to monitor are the absence of transmissions, the successful transmissions and the collisions [31]. However, the Rivest algorithm needs also to estimate the number of active stations (also referred to as *backlog*), and to this end he defined a complex pseudo-Bayesian strategy to estimate the backlog in a Slotted-Aloha-type channel. In the Rivest work, by assuming that collisions, successful transmissions, and idle slots have the same length (equal to one slot), it is shown that the maximum throughput is obtained by setting the transmission probability of each station equal to $1/\tilde{M}$, where \tilde{M} is an estimate of the number of active stations. The Rivest approach does not apply to a general slotted system. In a general slotted system, messages may have a length of several slots, and this implies that the maximum throughput is not obtained using a transmission probability equal to $1/\tilde{M}$. A pseudo-Bayesian approach, similar to the Rivest approach, has been proposed in [2] for a CSMA/CA network in which the ratio between the length of idle slots and messages is very small. One of the main limitations in the Rivest approach is the need to estimate the number of active stations because it is extremely complex to obtain a robust estimate of the number of active stations in a random access protocol. Specifically, Rivest assumes that, for a large network population, the \tilde{M} distribution is well approximated by a Poisson distribution. The Poisson model is an approximation to a large but finite population in which each station generates messages infrequently and each message can be successfully transmitted in a time interval much shorter

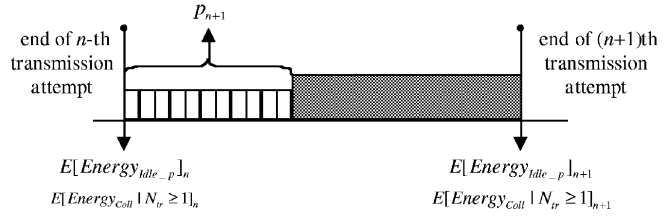


Fig. 8. The $(n + 1)$ th transmission interval.

than the average time between successive messages generated by a given station. The current usage scenarios for the wireless local area networks impose not considering anymore the networks as lightly loaded and each station as a source of sparse messages. These considerations motivate the need to propose an innovative transmission control strategy that well adapts to the current nature of traffic loads in the wireless networks. For this purpose, in this paper, we have carried out the analysis of *p*-persistent CSMA access schemes by adopting a finite population model constituted by stations that have always a message waiting to be transmitted, as during a typical file transfer. This study allows us to afford the issue of developing algorithms for the optimization of the protocol performances within more realistic scenarios.

4.2 A Feedback-Based Strategy to Achieve Power-Saving/Efficiency Optimization in *p*-Persistent CSMA Access Schemes

Equation (14) provides the criteria that must be satisfied, after each transmission attempt, to approach the minimum Energy Consumption. To achieve this, our protocol updates the transmission probability adopted by each station to balance the energy consumed during idle periods and collisions. Hereafter, we denote as *transmission interval* the time interval between two consecutive transmission attempts.

To better clarify the operations performed by a station, let us refer to Fig. 8. Specifically, the figure presents the station behavior during the $(n + 1)$ th transmission interval, i.e., the time interval between the end of the n th transmission attempt and the end of $(n + 1)$ th transmission attempt.

We assume that at the beginning of $(n + 1)$ th transmission interval, i.e., at the end of the n th transmission attempt, each station has the following information:

- p_n is the transmission probability adopted by all the station in the network during the n th transmission interval.
- $E[Energy_{Idle-p}]_n$ is the estimate (at the end of the n th transmission interval) of the average energy consumed during idle periods.
- $E[Energy_{Coll} | N_{tr} \geq 1]_n$ is the estimate (at the end of the n th transmission interval) of the average energy consumed during collisions.

If $p_n \neq p_{opt}^E$, (14) does not hold and

$$E[Energy_{Idle-p}]_n \neq E[Energy_{Coll} | N_{tr} \geq 1]_n.$$

For the $(n + 1)$ th transmission interval our algorithm searches a new transmission probability p_{n+1} such as to have $E[Energy_{Idle-p}]_n = E[Energy_{Coll} | N_{tr} \geq 1]_n$, i.e., to balance (in the future) the energy consumed during idle periods and collisions. Obviously, if

$$E[Energy_{Idle-p}]_n > E[Energy_{Coll}|N_{tr} \geq 1]_n,$$

we should increase the p value of a given percentage, otherwise we should decrease it. Hence, the new transmission probability p_{n+1} can be expressed as a function of p_n and an unknown quantity x , such that:

$$p_{n+1} = p_n(1 + x). \quad (23)$$

From the closed formula of

$$E[Energy_{Idle-p}]_n$$

and

$$E[Energy_{Coll}|N_{tr} \geq 1]_n$$

(provided by Lemma 1), we might derive the unknown $(1 + x)$ quantity by substituting formula (23) in (14). However, this procedure is unfeasible because it requires the knowledge of M . In addition, these formulas do not yield to a closed formula for the $(1 + x)$ quantity. To overcome this issues, we rewrite (14) to provide a simpler, even though approximate expression. By proceeding in this way, in the following Lemma, we provide the $(1 + x)$ quantity by assuming $Mp_n \ll 1$.⁶

Lemma 3. *In a M -station network that adopts a p -persistent CSMA access scheme, if $Mp_n \ll 1$, and by assuming that the network is not far from the stationary conditions, then*

$$p_{n+1} = p_n(1 + x),$$

where

$$(1 + x) = \frac{\sqrt{1 + 4(1 + E[Idle-p]_n) \frac{E[Energy_{Coll}|N_{tr} \geq 1]_n}{PRX}} - 1}{\frac{2E[Energy_{Coll}|N_{tr} \geq 1]_n}{PRX}}, \quad (24)$$

$E[Idle-p]_n$ denotes the estimate, at the end of the n th transmission interval, of the average number of consecutive empty slots, and $E[Energy_{Coll}|N_{tr} \geq 1]_n$ denotes the estimate, at the end of the n th transmission interval, of the average energy consumed by a generic station during collisions.

Proof. The proof is based on the same line of reasoning adopted for the proof of Lemma 2. We assume that p_{opt}^E is identified by (14) and that (15.a) and (15.b) hold. Under the condition $Mp_n \ll 1$, the following polynomial approximation can be adopted:

$$(1 - p)^M = 1 - Mp + O((Mp)^2) \xrightarrow{Mp \gg 1} 1 - Mp. \quad (25)$$

Furthermore, under the same condition $Mp_n \ll 1$, (19.b) and (19.c) also hold. By exploiting (25), (15.a), (15.b), (19.b), and (19.c), we can write:

$$E[Energy_{Idle-p}]_n \approx PRX \cdot \frac{1 - Mp_n}{Mp_n}, \quad (26.a)$$

$$E[Energy_{Coll}|N_{tr} \geq 1]_n \approx \bar{E}_{CT} \cdot \frac{(M-1)}{2M} p_n + \bar{E}_{CNT} \cdot \frac{(M-1)(M-2)}{2M} p_n. \quad (26.b)$$

To derive the $(1 + x)$ quantity, we impose that (14) holds at the end of $(n + 1)$ th transmission attempt. Hence, by exploiting (26.a) and (26.b), and assuming that $p_{n+1} = p_n(1 + x)$, (14) can be written as:

$$PRX \cdot \frac{1 - Mp_n(1 + x)}{Mp_n} = \left[\bar{E}_{CT} \cdot \frac{(M-1)}{2M} p_n + \bar{E}_{CNT} \cdot \frac{(M-1)(M-2)}{2M} p_n \right] \cdot (1 + x)^2. \quad (27)$$

By noting that the first term in the right-hand side of (27) is $E[Energy_{Coll}|N_{tr} \geq 1]_n$, and by exploiting relationship (26.a) to express the Mp_n product, we obtain:

$$PRX \cdot \frac{1 - \frac{(1+x)}{1+E[Idle-p]_n}}{\frac{1}{1+E[Idle-p]_n}} = E[Energy_{Coll}|N_{tr} \geq 1]_n \cdot (1 + x)^2. \quad (28)$$

By solving (28), (24) is obtained and this concludes the proof. \square

Formula (24) provides the updating rule for the transmission probability that our transmission control strategy implements to approach the minimum Energy Consumption. However, a real implementation of the proposed protocol requires that the $E[Idle-p]_n$ and $E[Energy_{Coll}|N_{tr} \geq 1]_n$ expressions are substituted with estimates of the average energy consumed during idle periods and collisions. In the following, we will show how these estimates can be obtained by exploiting the carrier sensing mechanism. To better clarify the way we obtain the $E[Energy_{Idle-p}]_n$ and $E[Energy_{Coll}|N_{tr} \geq 1]_n$ estimates, we refer to the Fig. 9, where we present the updating procedure adopted, and the feedback information from the channel status we utilize.

Each station, by using the carrier sensing mechanism, can observe the channel status and measure the length of idle periods and busy periods. In the latter case, we assume that it can distinguish successful transmissions from collisions by observing the ACK. Among collisions, each station obviously knows the collisions in which it is involved or not. From these values, $E[Idle-p]_n$, $E[Energy_{tag_Coll}|N_{tr} \geq 1]_n$, and

$$E[Energy_{not_tag_Coll}|N_{tr} \geq 1]_n (E[Energy_{Coll}|N_{tr} \geq 1]_n$$

is simply the sum of

$$E[Energy_{tag_Coll}|N_{tr} \geq 1]_n$$

and

$$E[Energy_{not_tag_Coll}|N_{tr} \geq 1]_n$$

can be approximated by exploiting a moving average window:

$$E[Idle-p]_n = \alpha \cdot E[Idle-p]_{n-1} + (1 - \alpha) \cdot Idle-p_n, \quad (29.a)$$

6. Let us remind that the numerical results shown in Figs. 3a and 3b confirm the accuracy of this assumption, at least in the optimal energy state and for $M \geq 10$.

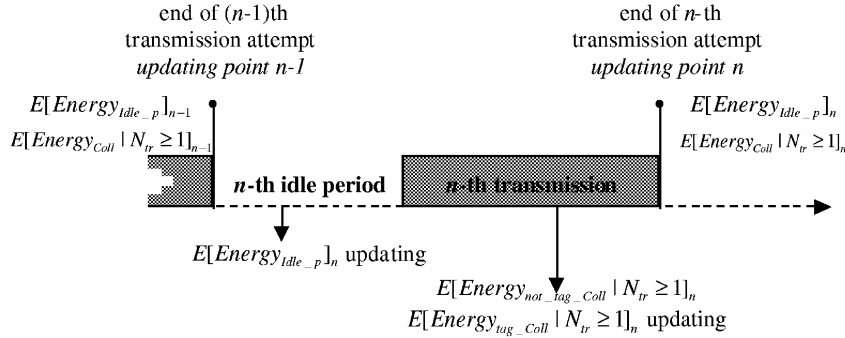


Fig. 9. Estimates updating.

$$\begin{aligned}
 E[Energy_{tag_Coll} | N_{tr} \geq 1]_n &= \alpha \cdot E[Energy_{tag_Coll} | N_{tr} \geq 1]_{n-1} \\
 &+ (1 - \alpha) \cdot [PTX \cdot Coll_{tagged}_n \\
 &+ PRX \cdot \max(0, Coll_n - Coll_{tagged}_n)],
 \end{aligned} \tag{29.b}$$

$$\begin{aligned}
 E[Energy_{not_tag_Coll} | N_{tr} \geq 1]_n &= \\
 \alpha \cdot E[Energy_{not_tag_Coll} | N_{tr} \geq 1]_{n-1} &+ (1 - \alpha) \cdot PRX \cdot Coll_{not_tagged}_n,
 \end{aligned} \tag{29.c}$$

where:

- $E[Idle_p]_n$, $E[Energy_{tag_Coll} | N_{tr} \geq 1]_n$, and $E[Energy_{not_tag_Coll} | N_{tr} \geq 1]_n$ are the approximations at the end of the n th transmission attempt.
- $Idle_p_n$ is the length of the n th idle period.
- $Coll_n$ is zero if either the n th transmission attempt is successful or a not tagged-station collision, otherwise, it is the collision length.
- $Coll_{tagged}_n$ is zero if either the n th transmission attempt is successful or a not tagged-station collision, otherwise, it is length of the tagged-station transmission.

- $Coll_{not_tagged}_n$ is zero if either the n th transmission attempt is successful or a tagged-station collision, otherwise, it is the collision length.
- α ($\alpha \in [0, 1]$) is a smoothing factor.

The use of a smoothing factor α is widespread in the network protocols to obtain reliable estimates from the network measures by avoiding harmful fluctuations. In the Table 6, we summarize the steps performed independently by each station to compute the p_{n+1} value for the current network and load conditions, given the p_n value.

To conclude this section, we will describe how (24) changes when the target of the transmission control strategy is the protocol capacity optimization, rather than the Energy Consumption minimization. The simplest way to modify the (24) is to assume $PTX/PRX = 1$ and rewrite accordingly (24). With this approach, we obtain that the updating rule for the p_n value that permits to attain the protocol capacity is:

$$(1 + x) = \frac{\sqrt{1 + 4(1 + E[Idle_p]_n)E[Coll | N_{tr} \geq 1]_n} - 1}{2E[Coll | N_{tr} \geq 1]_n}. \tag{30}$$

The tight analogy between (24) and (30) is evident: The latter can be considered as a special case of the former.

TABLE 6
Description of Our Transmission Control Strategy

<p>Begin</p> <p>step 1: measure of the n-th the idle period $Idle_p_n$;</p> <p>step 2: measure of $Coll_n$, $Coll_{tagged}_n$ and $Coll_{not_tagged}_n$;</p> <p>step 3: update of $E[Idle_p]_n$, $E[Energy_{tag_Coll} N_{tr} \geq 1]_n$ and $E[Energy_{not_tag_Coll} N_{tr} \geq 1]_n$ [by exploiting (29.a) to (29.c)]</p> <p>step 4: calculate</p> $p_{new} = p_n \cdot \frac{\sqrt{1 + 4(1 + E[Idle_p]_n) \left(\frac{E[Energy_{tag_Coll} N_{tr} \geq 1]_n + E[Energy_{not_tag_Coll} N_{tr} \geq 1]_n}{PRX} \right)} - 1}{2 \left(\frac{E[Energy_{tag_Coll} N_{tr} \geq 1]_n + E[Energy_{not_tag_Coll} N_{tr} \geq 1]_n}{PRX} \right)}$ <p>step 5: $p_{n+1} = \alpha \cdot p_n + (1 - \alpha) \cdot p_{new}$;</p> <p>End</p>
--

5 ENHANCEMENTS OF THE IEEE 802.11 MAC PROTOCOL: PERFORMANCE ANALYSIS

In this section, we adapt the analytical framework developed in Sections 2 and 3 to a specific implementation of the *p-persistent* CSMA access scheme: the *p-persistent* IEEE 802.11 protocol [12]. In addition, we enhance the *p-persistent* IEEE 802.11 protocol with the feedback-based strategy defined in Section 4. Let us remind that the *p-persistent* IEEE 802.11 protocol performances, from both the capacity and Energy Consumption standpoint, correspond to the performances of the standard IEEE 802.11 protocol [4], [12], [8]. It may be argued that the IEEE 802.11 protocol does not use a *p-persistent* backoff algorithm and that the tuning of its backoff window size is obtained at the cost of collisions. However, we wish to point out that *p-persistent* IEEE 802.11 results can be exploited also to enhance the standard IEEE 802.11 protocol. Several solutions can be devised which are still based on the binary exponential backoff of the standard and use the knowledge of the optimal window size (i.e., the window size that corresponds to the optimal *p* value [12]) to improve its performance. For example, a solution can be organized in two steps. In the first step, the binary exponential backoff of the standard is used to identify the slot in which a given transmission could occur (i.e., the slot corresponding to a backoff counter equal to 0). In the second step, the optimal window size criteria is applied to determine if it is wise to use the identified slot or it is better to defer the transmission [6].

5.1 Capacity and Energy Consumption Analysis of the *p-Persistent* IEEE 802.11 Protocol

The *p-persistent* IEEE 802.11 protocol belongs to the general family of *p-persistent* CSMA access schemes; however, it differentiates from other *p-persistent* protocols for the overheads introduced to satisfy the requirements imposed by the physical layer adopted in the IEEE 802.11 standard. Specifically, a station cannot initiate a transmission as soon as it senses the channel idle, but only after the medium is found to be idle for an interval that exceeds the *Distributed InterFrame Space* (DIFS). On the other hand (i.e., the medium is busy), the transmission is deferred until the end of the ongoing transmission. The decision of beginning a transmission in the time slot following a DIFS idle interval or to defer the transmission to the next time slots is accomplished according to the transmission probability *p*. A further significant difference with the protocol behavior described in Section 2.1 is the introduction of the acknowledgement traffic. Specifically, immediate positive acknowledgements are employed to ascertain the successful reception of each message transmission. This is accomplished by the receiver (immediately following the reception of the data frame), which initiates the transmission of an acknowledgement message, say ACK, after a time interval referred to as *Short InterFrame Space* (SIFS), which is less than DIFS. If an acknowledgement is not received, the data frame is presumed to have been lost and a retransmission is scheduled, after a time interval referred to as *Extended InterFrame Space* (EIFS), which is greater than DIFS. Furthermore, to support the MAC services defined in [28], each data frame is constituted by: 1) a *MAC header*, say MAC_{hdr} , which contains the MAC addresses and control information, 2) a variable length *data payload*,

which contains the data information, and 3) a *frame error sequence* (FCS), for error detection. Finally, to support the physical procedures of transmission (carrier sense and reception) a *physical layer preamble* (PLCP preamble) and a *physical layer header* (PLCP header) have to be added to both data and control frames. Hereafter, we will refer to the sum of PLCP preamble and PLCP header as PHY_{hdr} . According to the *p-persistent* IEEE 802.11 protocol behavior, the average length of a successful transmission is increased with respect to the $l \cdot t_{slot}$ considered in (1). Specifically, by denoting with τ the maximum propagation delay between two WLAN stations, the average time required to complete a successful transmission includes the following additional overhead [12]:

$$IEEE802.11_overhead_success = 2\tau + SIFS + ACK + DIFS \quad (31)$$

while the following overhead must be added to each collision:

$$IEEE802.11_overhead_collision = \tau + EIFS. \quad (32)$$

Hence, by assuming that the average data payload length is $l \cdot t_{slot}$, according to the protocol behavior, we have:

$$E[Succ | N_{tr} \geq 1] PHY_{hdr} + MAC_{hdr} + l \cdot t_{slot} + FCS + IEEE802.11_overhead_success, \quad (33.a)$$

$$E[Transmission\ attempt | N_{tr} \geq 1] = E[Succ | N_{tr} \geq 1] \cdot P_{Succ | N_{tr} \geq 1} + [PHY_{hdr} + MAC_{hdr} + E[Coll | Collision] + FCS + \tau + EIFS] \cdot P_{Coll | N_{tr} \geq 1}. \quad (33.b)$$

It is also worth noting that, when we analyze the Energy Consumption, the overheads defined by (31) and (32) must be multiplied by PRX , as those overheads represent a time interval during which the tagged station is in the receiving state. At the same way, the MAC_{hdr} and PHY_{hdr} must be multiplied by either PTX or PRX according to whether the frame is transmitted by the tagged station or a not-tagged station. Hence, the formula for the Energy Consumption in the *p-persistent* IEEE 802.11 protocol is simply obtained by adding the corresponding overheads to the formulas of the energy consumed during successes and collisions and, thus, are not reported here.

Hereafter, we will indicate as *Power Saving* (PS)-*Efficient* IEEE 802.11 protocol the *p-persistent* IEEE 802.11 protocol enhanced by the transmission control strategy based on the runtime estimate of the p_{opt}^E value defined in Section 4.2. The performances achieved by the PS-Efficient IEEE 802.11 protocol will be investigated via simulation and compared with those of the standard IEEE 802.11 protocol ([28], [10]). The numerical results presented in the next sections depend on the specific setting of the IEEE 802.11 protocol parameters. Table 7 gives the values for the protocol parameters adopted in our simulation runs. It is worth pointing out that this parameter setting is compliant with the operating setting for the Frequency Hopping Spread Spectrum physical layer at 2 Mbps of the standard IEEE 802.11 protocol [28].

TABLE 7
p-Persistent IEEE 802.11 Configuration

t_{slot}	τ	PHY_{hdr}	MAC_{hdr}	FCS	$Bit\ Rate$
50 μ sec	$\leq 1 \mu$ sec	128 bits ($2.56 t_{slot}$)	240 bits ($2.4 t_{slot}$)	32 bits ($0.32 t_{slot}$)	2Mbps
DIFS	SIFS	ACK		CW_{MIN}	CW_{MAX}
$2.56 t_{slot}$	$0.56 t_{slot}$	112 bits + PHY_{hdr}		$8 t_{slot}$	$256 t_{slot}$

Results presented hereafter, are obtained with a geometric message-length distribution. Similar results have been derived for the other message-length distributions [10]. In all the simulations carried out, the users operate in asymptotic conditions. Furthermore, we assume an ideal channel with no transmission errors and no hidden terminals, i.e., each station can always hear all the others.

We investigate the PS-Efficient IEEE 802.11 protocol behavior both in stationary and transient conditions. Steady-state performance figures have been estimated with the independent replication technique with a 90 percent confidence level. Confidence intervals are not reported into the graphs as they are always very tight (≤ 1 percent).

5.2 PS-Efficient IEEE 802.11 Performance Analysis in Steady State

In this section, we will exhaustively validate the capacity of the PS-Efficient IEEE 802.11 to closely approach the optimal Energy Consumption in a network with a stationary configuration, i.e., the M value is constant.

In Figs. 10a, 10b, 10c, and 10d, we compare, for several network configurations ($M \in [5 \dots 100]$), the Energy Consumption of the standard IEEE 802.11 protocol (STD 802.11) and of the PS-Efficient IEEE 802.11 protocol (PS-E 802.11) with the theoretical lower bound of the Energy Consumption (OPT 802.11). Figs. 10a and 10b show the results corresponding to networks where short messages are transmitted (average message length $l = 2t_{slot}$).⁷ In Figs. 10c and 10d, we report the same results by assuming that long messages are transmitted (average message length $l = 100t_{slot}$). For each network and traffic configuration, we consider two different network-interface settings: $PTX/PRX = 2$ and $PTX/PRX = 10$. The logarithmic scale for the y -axis has been chosen to better highlight the Energy Consumption behavior for both the low values measured within small network-size populations and the high values measured within large network-size populations.

The curves related to the PS-Efficient IEEE 802.11 Energy Consumption overlap the theoretical lower bound in all the configurations analyzed. Therefore, the numerical results clearly show that the effectiveness of PS-Efficient IEEE 802.11 protocol does not depend on the number of active stations and the messages' lengths. Furthermore, by analyzing the curves obtained with $PTX/PRX = 2$ and $PTX/PRX = 10$, it results that the effectiveness of the PS-Efficient IEEE 802.11 protocol is also independent by the network-interface power consumption. For the PS-Efficient

IEEE 802.11 protocol, we have considered different smoothing factors to investigate the impact of the memory-estimate length on the protocol performances. The numerical results show that the PS-Efficient IEEE 802.11 protocol becomes closer to the theoretical lower bound for the Energy Consumption if we increase the α values. However, the differences between the Energy Consumption figures measured are not meaningful and they cannot be appreciated from the figures [10]. Finally, by comparing Figs. 10a and 10b with Figs. 10c and 10d, respectively, we observe that there are not differences in the ability of the PS-Efficient IEEE 802.11 protocol to approach the optimal performance both with short messages and with long messages.

Since through the analytical study we have shown that the optimal average number of transmitting stations is strongly affected by the average message length, we have performed a second set of simulations to better analyze the PS-Efficient IEEE 802.11 dependency on the message length. Specifically, in Figs. 11a, 11b, 11c, and 11d, we compare (by varying the average data payload length ($l \in [2 \dots 100]$)) the Energy Consumption of the two protocols (standard IEEE 802.11 and PS-Efficient IEEE 802.11) with the theoretical lower bound of the Energy Consumption. Figs. 11a and 11b (Figs. 11c and 11d) show the results related to small (large) network-size populations, i.e., $M = 10$ ($M = 100$). For each network and traffic configuration, we consider two different network interface settings, i.e., $PTX/PRX = 2$ and $PTX/PRX = 10$. The curves related to the PS-Efficient IEEE 802.11 Energy Consumption overlap all the configurations analyzed thus showing the effectiveness of PS-Efficient IEEE 802.11 protocol. Furthermore, the obtained results show that the effectiveness of PS-Efficient IEEE 802.11 protocol does not depend on: the average message length, the number of active stations, and the network interface characteristics. In addition, also the α value has a low impact on the performance of the PS-Efficient IEEE 802.11 protocol. By increasing the α value, the PS-Efficient IEEE 802.11 protocol becomes closer to the theoretical lower bound for the Energy Consumption. However, the curves corresponding to different α values are always very close and almost no difference can be observed in the figures.

5.3 PS-Efficient IEEE 802.11 Performance Analysis in Transient Conditions

The performance analysis carried out so far assumed a network in stationary conditions. In particular, we have assumed that the number of stations in the network is fixed. This assumption has allowed us to verify the effectiveness of the PS-Efficient IEEE 802.11 protocol in steady state conditions. However, in the introduction, we have highlighted that one of the most critical issues in the design of wireless networks is the dynamic topology. Therefore, in the following analysis, we will investigate the PS-Efficient IEEE 802.11 ability to react to changes in the number of active stations.

Figs. 12a and 12b show the Energy Consumption (for an average message length $l = 2t_{slot}$) measured in the standard IEEE 802.11 protocol (STD 802.11) and the PS-Efficient IEEE 802.11 protocol (PS-E 802.11) against the theoretical lower bounds of the Energy Consumption (OPT 802.11). In the figures, we report two values for the theoretical lower bounds of the Energy Consumption: corresponding to 10

7. It is worth noting that at the 2-Mbps rate a single slot can contain up to 100 bits of information.

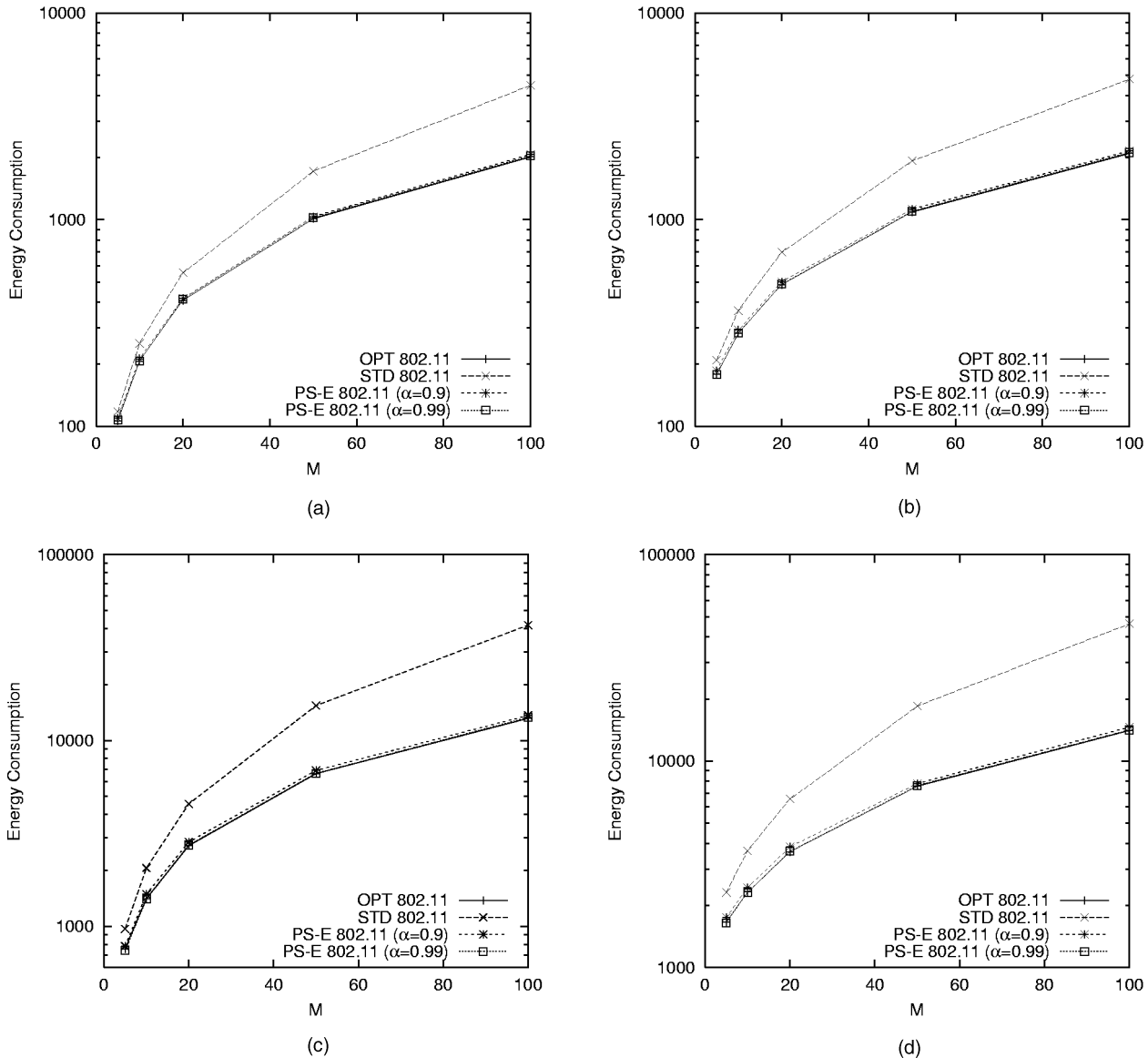


Fig. 10. Energy Consumption versus the number of stations in the network. (a) $l = 2t_{slot}$ and $PTX/PRX = 2$. (b) $l = 2t_{slot}$ and $PTX/PRX = 10$. (c) $l = 100t_{slot}$ and $PTX/PRX = 2$. (d) $l = 100t_{slot}$ and $PTX/PRX = 10$.

and 100 active stations, respectively. The Energy Consumption is measured during consecutive (not overlapping) time intervals. Hereafter, a time interval corresponds to $2048t_{slot}$ (i.e., 102 msec). In these evaluations, we assume that at time 0 the network is in steady-state with 10 active stations. After 50 time intervals, the number of stations in the network sharply increases to 100, causing the contention level to significantly increase. After 100 time intervals, the number of stations sharply comes back to the initial number of 10 stations. The figures show that the PS-Efficient 802.11 protocol promptly reacts to the contention-level changes. Specifically, in the PS-Efficient 802.11 protocol, the Energy Consumption always remains close to its optimal value. To better highlight the Energy Consumption behavior for both the low values measured within small network-size populations and the high values measured within large network-size populations, we have used the logarithmic scale on the y-axis. We can observe that the standard 802.11 protocol, when in the network there are 100 stations, shows

an Energy Consumption that is about two times the one measured in the PS-Efficient 802.11 protocol. Furthermore, the Energy Consumption is much more variable in the standard protocol than in the enhanced one.

The numerical results shown in Figs. 12a and 12b are related to $PTX/PRX = 2$ and $PTX/PRX = 10$, respectively. How extensively explained in Section 3, the impact of the PTX value on the Energy Consumption is more significant for small network-size populations. This effect is clearly shown also in Figs. 12a and 12b, where the Energy Consumption measured when in the network there are 100 stations with both $PTX/PRX = 2$ and $PTX/PRX = 10$ are similar. It is worth pointing out that the Energy Consumption behavior measured in the standard IEEE 802.11 protocol is independent of the PTX/PRX values because the standard protocol is not adaptive to the network interface characteristics, but only to the contention level. Hence, the number and length of collisions we observe in the standard IEEE 802.11 protocol

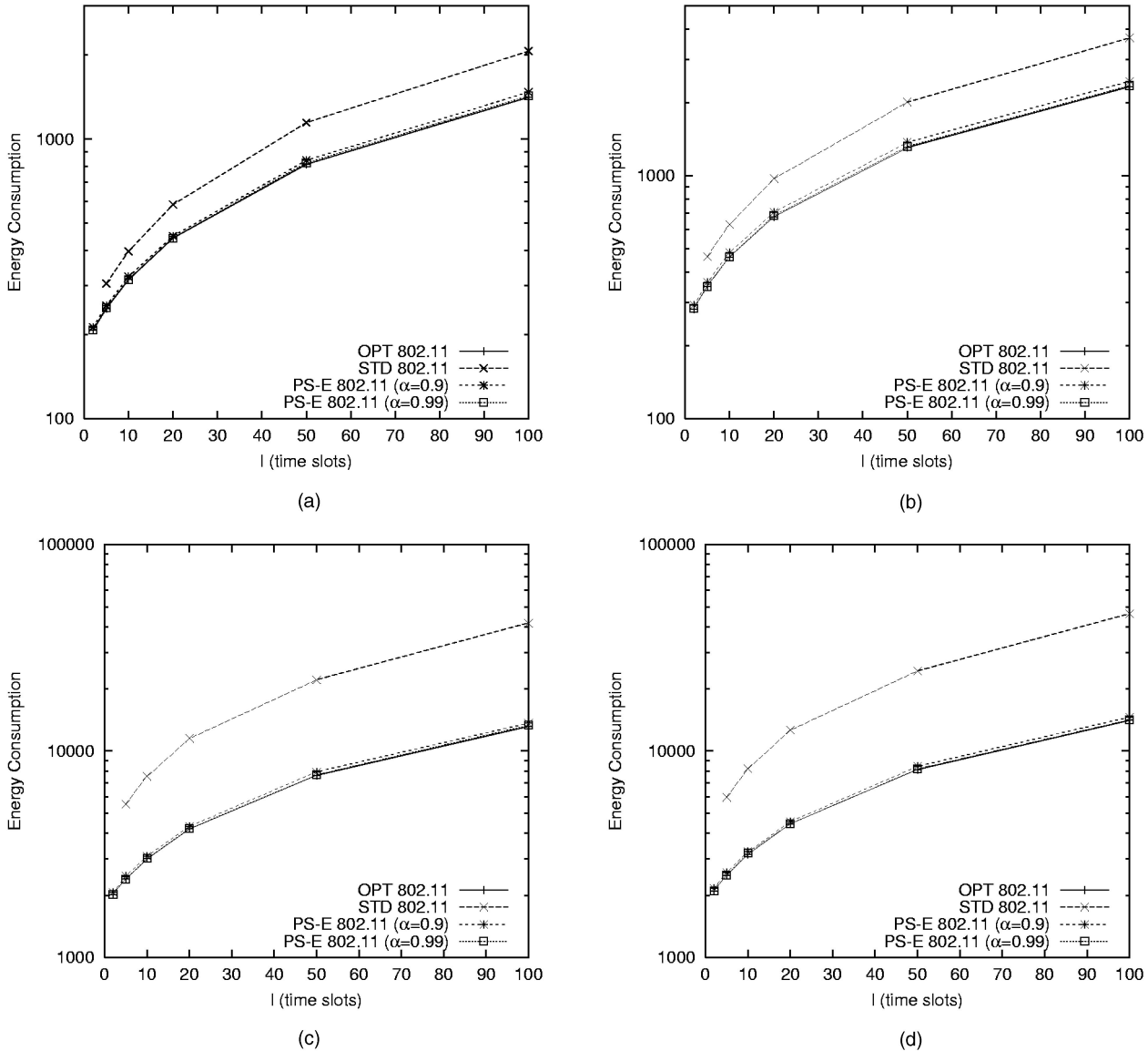


Fig. 11. Energy Consumption versus the average data payload length. (a) $M = 10$ and $PTX/PRX = 2$. (b) $M = 10$ and $PTX/PRX = 10$. (c) $M = 100$ and $PTX/PRX = 2$. (d) $M = 100$ and $PTX/PRX = 10$.

during the two simulation traces for $PTX/PRX = 2$ and $PTX/PRX = 10$ are the same.

The previous scenario (the M value sharply changes) analyzes the behavior of the PS-Efficient 802.11 protocol in an extreme situation. However, one may argue that in a more realistic situation, each station alternates between active and idle periods and, hence, the number of active-station changes in a continuous way. To model this scenario, we assumed that after each successful transmission a station decides according to a fixed probability p_i to enter an *inactivity* period.⁸ Results obtained with this active-idle model are presented in Figs. 13a and 13b. Specifically, in these figures, we plot the Energy Consumption in a network with 50 stations that follow the active-idle model. The p_i value is chosen to guarantee that the average number of active stations is 25. In Fig. 13, the straight line labeled

“OPT 802.11” represents the optimal value in a network with 25 stations operating in asymptotic conditions, i.e., always active. The curves clearly show that the performance figure of the PS-Efficient 802.11 protocol oscillates around the optimal value,⁹ while the standard protocol is always less efficient and often operates very far from the optimal point.

5.4 MAC Delay Analysis

In the previous performance analysis, we have focused on the Energy Consumption. In this section, we want to concentrate on the MAC delay¹⁰ measured both in the standard IEEE 802.11 (STD 802.11) and in the PS-Efficient IEEE 802.11 (PS-E 802.11) protocol.

It is straightforward to note that, due to the asymptotic load assumption, a transmission control strategy that

9. Fluctuations are due to the variable number of active stations.

10. Let us remind that the MAC delay is defined as the time required to successfully transmit the message that is at the top of a station's queue [16].

8. The inactivity time period has a geometric distribution with an average equal to two time intervals.

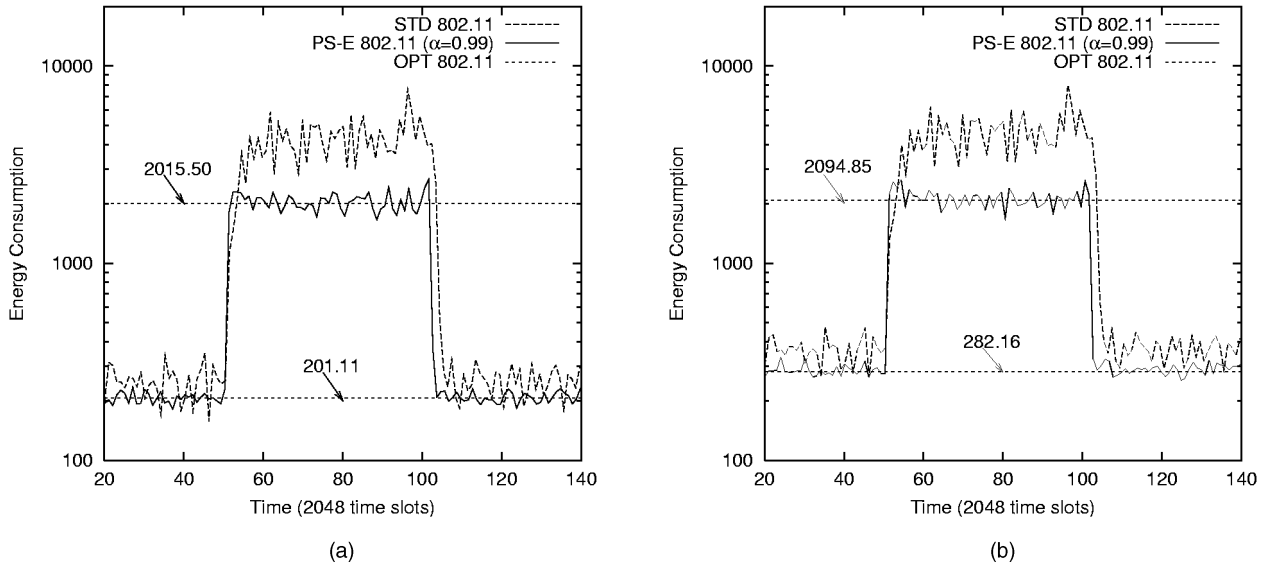


Fig. 12. Dynamic Energy Consumption with M -value sharp changes. (a) $l = 2t_{slot}$ and $PTX/PRX = 2$. (b) $l = 2t_{slot}$ and $PTX/PRX = 10$.

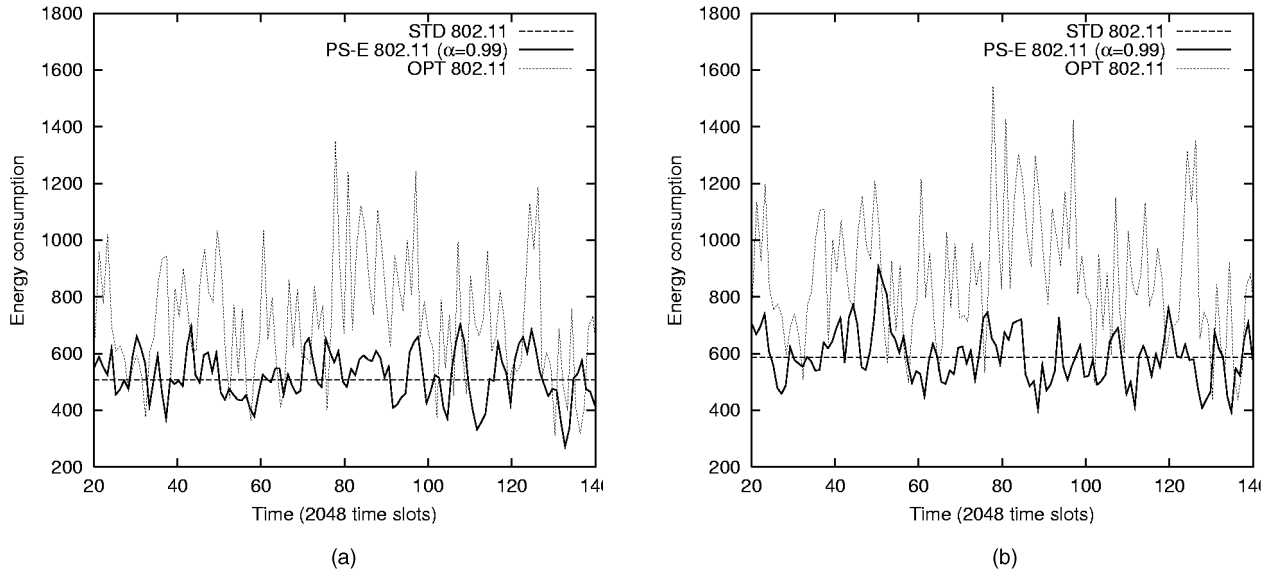


Fig. 13. Dynamic Energy Consumption with small but frequent change of the M value. (a) $l = 2t_{slot}$ and $PTX/PRX = 2$. (b) $l = 2t_{slot}$ and $PTX/PRX = 10$.

maximizes the average channel utilization also minimizes the average MAC delay. However, we cannot deduce from the throughput figures the characteristics of the MAC delay distributions. Furthermore, no information on the average MAC delay is available when the minimization of the Energy Consumption is our target. In principle, in the attempt to minimize the Energy Consumption, the tagged-station may spend more time in the idle state than the standard protocol. This may produce longer MAC delays in PS-E 802.11 with respect to the standard. These considerations motivate the need to investigate through simulations the MAC delay performances in the PS-Efficient IEEE 802.11 protocol.

In Tables 8 and 9, we compare the average 99th percentile and 999th percentile for the MAC delay distribution in STD 802.11 and in PS-E 802.11. The network has 100 active stations. We have considered both short messages (i.e.,

$l = 2t_{slot}$) and long messages (i.e., $l = 100t_{slot}$). We report the results only for $PTX/PRX = 2$ because there are not meaningful differences with the results obtained with $PTX/PRX = 10$. The numerical results show that there is a significant improvement also in the MAC delay performances when we adopt our transmission control strategy that computes at runtime the p_{opt}^E value. Specifically, with PS-E 802.11, we have (with respect to the STD 802.11) a reduction in the average MAC delay and a shorter tail for

TABLE 8
MAC Delay ($l = 2t_{slot}$ and $PTX/PRX = 2$)

	Average MAC Delay	99 th Percentile	999 th percentile
STD 802.11	216.88 (msec)	1750(msec)	2950(msec)
PS-E 802.11	100.66 (msec)	245 (msec)	675 (msec)

TABLE 9
MAC Delay ($l = 100t_{slot}$ and $PTX/PRX = 2$)

	Average MAC Delay	99 th Percentile	999 th percentile
<i>STD 802.11</i>	1.91953 (sec)	16.2 (sec)	25.5 (sec)
<i>PS-E 802.11</i>	0.65629 (sec)	3.05(sec)	4.8 (sec)

the MAC delay distribution. From this analysis, we can assess that our transmission control strategy achieves its target (i.e., energy consumption minimization) without degrading the quality of service experienced by the network stations. Indeed, our feedback-based strategy, by reducing the network contention level, has a positive effect also on the quality of service by contributing to reduce the time it takes to successfully transmit a packet.

6 CONCLUSIONS

This paper focuses on the analysis and optimization of the two main performance figures for a WLAN: the throughput and power consumption. The main contributions of the paper are: 1) the analytical characterization of the relationship between the protocol parameters and the selected performance figures and 2) simple (yet precise) approximate relationships to characterize the optimal operating points from the efficiency and power consumption standpoints. By exploiting items 1 and 2, we have designed a feedback-based algorithm to dynamically tune the protocol to achieve its optimal performance. Our algorithm estimates the collision and idle period costs and (by adopting the analytical framework we have developed) computes the p value that equates these costs. The idea to use the above events for estimating the number of active stations (also referred to as backlog) was also proposed by Rivest for S-ALOHA protocols. The approach we present in this paper is more general as: 1) it is suitable for a larger class of protocols and 2) it can be used to optimize (in some cases at the same time), beyond the throughput, the energy consumption.

As far as item 1 in the above paragraph is concerned, it is worth noting that our algorithm does not require any assumption on the length of idle slots, messages, and collisions. In addition, it adopts a more realistic population model. Specifically, Rivest assumes a large network population in which each station generates messages infrequently. In this paper, we adopt a finite population model constituted by stations that always have a message waiting to be transmitted, as during a typical file transfer. This model provides an adequate representation of the current usage scenarios for LANs. An additional innovative and important feature of our algorithm is that it does not require any estimations of the number of active stations. This estimation, in a dynamic WLAN environment, is complex to achieve and it is prone to errors.

The hidden-station phenomenon is not considered in this paper. The IEEE 802.11 standard has an optional mechanism (RTS/CTS) which must be used whenever the hidden station phenomenon occurs frequently. Extension of the mechanism for the dynamic tuning of the backoff algorithm when RTS/CTS mechanism is operating is an ongoing research activity.

APPENDIX A

Lemma A.1. *In a M -station network that adopts a p -persistent CSMA access scheme, by assuming that each station is operating in asymptotic conditions and the sequence of message lengths $\{L_i\}$, normalized to t_{slot} , are i.i.d. random variables:*

$$E[Idle_p] = t_{slot} \cdot \frac{(1-p)^M}{1-(1-p)^M}, \quad P_{Succ|N_{tr} \geq 1} = \frac{Mp(1-p)^{M-1}}{1-(1-p)^M},$$

$$P_{Coll|N_{tr} \geq 1} = \frac{1 - \left[(1-p)^M + Mp(1-p)^{M-1} \right]}{1(1-p)^M}$$

$$E[Coll|Collision] = \frac{t_{slot}}{1 - \left[(1-p)^M + Mp(1-p)^{M-1} \right]}$$

$$\sum_{h=1}^{\infty} h \left\{ [1 - (1 - P\{L \leq h\})p]^M - [1 - (1 - P\{L < h\})p]^M - M[P\{L \leq h\} - P\{L < h\}]p(1-p)^{M-1} \right\}.$$

Proof. For the proof of $E[Idle_p]$, $P_{Succ|N_{tr} \geq 1}$, and $P_{Coll|N_{tr} \geq 1}$ formulas, see [12]. Hereafter, we concentrate on the $E[Coll|Collision]$ derivation. The collision length, say $Coll$, depends on the number of colliding messages, N_{cp} , and it is equal to

$$Coll = \max\{L_1, L_2, \dots, L_{N_{cp}}\}, \quad (\text{A.1})$$

where L_i is the length of i th colliding message. Hence,

$$E[Coll|Collision] = t_{slot} \cdot \sum_{m=1}^{\infty} m \cdot \left[\sum_{n=2}^M P\{Coll = m|N_{cp} = n\} \cdot P\{N_{cp} = n|N_{cp} > 1\} \right], \quad (\text{A.2})$$

where:

$$P\{N_{cp} = n|N_{cp} > 1\} = \frac{\binom{M}{n} p^n (1-p)^{M-n}}{1 - \left[(1-p)^M + Mp(1-p)^{M-1} \right]}, \quad (\text{A.3})$$

and

$$P\{Coll = m|N_{cp} = n\} = P\{\max\{L_1, L_2, \dots, L_n\} = m\}. \quad (\text{A.4})$$

Equation (A.4) can be written as:

$$P\{\max\{L_1, L_2, \dots, L_n\} = m\} = \sum_{k=1}^n \binom{n}{k} [P\{L = m\}]^k [P\{L < m\}]^{n-k} - \sum_{k=0}^n \binom{n}{k} [P\{L = m\}]^k [P\{L < m\}]^{n-k} - [P\{L < m\}]^n. \quad (\text{A.5})$$

The first term in the r.h.s. of (A.5) is $[P\{Lm\}]^n$. By substituting (A.3) and (A.5) in (A.2), after some algebraic

manipulations, the closed formula for $E[Coll|Collision]$ as presented in Lemma A.1 is obtained. \square

APPENDIX B

- $E[Energy_{not_tag_Coll}|not_tag_Coll]$ approximation
By noting that:

$$E[Energy_{not_tag_Coll}|not_tag_Coll] = t_{slot} \cdot PRX \cdot \sum_{m=1}^{\infty} m \cdot \left[\sum_{n=2}^{M-1} P\{Coll = m|N_{cp} = n\} \cdot P\{N_{cp} = n|N_{cp} > 1\} \right], \quad (B.1)$$

and by assuming that no more than two stations are colliding at the same time, it follows:

$$E[Energy_{not_tag_Coll}|not_tag_Coll] \approx t_{slot} \cdot PRX \cdot \sum_{m=1}^{\infty} m \cdot \Pr\{\max\{L_1, L_2\} = m\}. \quad (B.2)$$

From the (B.2) definition, (15.a) can be written.

- $E[Energy_{tag_Coll}|not_tag_Coll]$ approximation
The energy required for a colliding tagged transmission is dependent on the length of the tagged transmission x , which determines the transmission power consumption. Hence,

$$E[Energy_{tag_Coll}|tag_Coll] = \sum_{x=1}^{\infty} E[Energy_{tag_Coll}|tag_Coll, tag_tr = x] \cdot \Pr\{tag_tr = x\}. \quad (B.3)$$

The additional duration of the collision after the colliding tagged transmission completion is dependent on the number i of the other colliding transmissions, hence:

$$E[Energy_{tag_Coll}|tag_Coll, tag_tr = x] = \sum_{i=1}^{\infty} E[Energy_{tag_Coll}|tag_tr = x, N_{other_tr} = i] \cdot \Pr\{N_{other_tr} = i|N_{other_tr} \geq 1\}. \quad (B.4)$$

By assuming that $\Pr\{N_{other_tr} = 1|N_{other_tr} \geq 1\} = 1$, (i.e., only one not tagged station collides with the tagged station) it follows that:

$$E[Energy_{tag_Coll}|tag_Coll] = \sum_{x=1}^{\infty} E[Energy_{tag_Coll}|tag_tr = x, N_{other_tr} = 1] \cdot \Pr\{tag_tr = x\}. \quad (B.5)$$

By denoting with z the length L of the not tagged transmission, we can write:

$$E[Energy_{tag_Coll}|tag_tr = x, N_{other_tr} = 1] = \sum_{z=1}^{\infty} E[Energy_{tag_Coll}|tag_tr = x, N_{other_tr} = 1, L = z] \cdot P\{L = z\}. \quad (B.6)$$

Finally,

$$E[Energy_{tag_Coll}|tag_tr = x, N_{other_tr} = 1] = PTX \cdot x + PRX \cdot \max(0, z - x). \quad (B.7)$$

From these definitions, with standard algebraic manipulations, (15.b) is obtained.

ACKNOWLEDGMENTS

The authors wish to express their gratitude to the anonymous referees. Their comments help to significantly improve the paper quality.

REFERENCES

- [1] N. Bambos, "Toward Power-Sensitive Network Architectures in Wireless Communications: Concepts, Issues, and Design Aspects," *IEEE Personal Comm.*, pp. 50-59, 1998.
- [2] D. Bertsekas and R. Gallager, *Data Networks*. Englewood Cliffs, N.J.: Prentice-Hall, 1992.
- [3] G. Bianchi, L. Fratta, and M. Olivieri, "Performance Evaluation and Enhancement of the CSMA/CA MAC Protocol for 802.11 Wireless LANs," *Proc. Personal Indoor Mobile Radio Conf. (PIMRC)*, pp. 392-396, 1996.
- [4] G. Bianchi, "IEEE 802.11—Saturation Throughput Analysis," *IEEE Comm. Letters*, vol. 2, no. 12, pp. 318-320, Dec. 1998.
- [5] G. Bianchi, "Performance Analysis of the IEEE 802.11 Distributed Coordination Function," *IEEE J. Selected Areas in Comm.*, vol. 18, no. 3, pp. 535-547, Mar. 2000.
- [6] L. Bononi, M. Conti, and E. Gregori, "Design and Performance Evaluation of an Asymptotically Optimal Backoff Algorithm for IEEE 802.11 Wireless LANs," *Proc. Hawaii Int'l Conf. System Sciences (HICSS-33)*, 2000.
- [7] L. Bononi, M. Conti, and L. Donatiello, "Design and Performance Evaluation of a Distributed Contention Control (DCC) Mechanism for IEEE 802.11 Wireless Local Area Networks," *J. Parallel and Distributed Computing*, vol. 60, no. 4, Apr. 2000.
- [8] L. Bononi, M. Conti, L. Donatiello, "A Distributed Mechanism for Power Saving in IEEE 802.11 Wireless LANs," *ACM/Kluwer Mobile Networks and Applications J.*, vol. 6, no. 3, pp. 211-222, 2001.
- [9] R. Bruno, M. Conti, and E. Gregori, "A Simple Protocol for the Dynamic Tuning of the Backoff Mechanism in IEEE 802.11 Networks," *Proc. European Wireless Conf. (EW2000)*, Sept. 2000.
- [10] R. Bruno, M. Conti, and E. Gregori, "Efficiency and Energy Consumption in IEEE 802.11 Wireless Local Area Networks," CNUCE Technical Report, July 2001.
- [11] R. Bruno, M. Conti, and E. Gregori, "Traffic Integration in Personal, Local and Geographical Wireless Networks," *Handbook of Wireless Networks and Mobile Computing*, chapter 7, I. Stojmenovic, ed., New York: John Wiley & Sons, 2001.
- [12] F. Cali, M. Conti, and E. Gregori, "Dynamic Tuning of the IEEE 802.11 Protocol to Achieve a Theoretical Throughput Limit," *IEEE/ACM Trans. Networking*, vol. 8, no. 6, pp. 785-799, Dec. 2000.
- [13] F. Cali, M. Conti, and E. Gregori, "Dynamic IEEE 802.11: Design, Modeling and Performance Evaluation," *IEEE J. Selected Areas in Comm.*, vol. 18, no. 9, pp. 1774-1786, Sept. 2000.
- [14] A. Chandra, V. Gumalla, and J.O. Limb, "Wireless Medium Access Control Protocols," *IEEE Comm. Surveys Second Quarter*, 2000.
- [15] J. Chen, K. Sivalingam, P. Agrawal, and S. Kishore, "A Comparison of MAC Protocols for Wireless Local Networks Based on Battery Power Consumption," *Proc. IEEE 17th Ann. Conf. Computer Comm. (Infocom '98)*, 1998.
- [16] M. Conti, E. Gregori, and L. Lenzini, "Metropolitan Area Networks," *Springer Verlag Limited Series Telecomm. Networks and Computer Systems*, Nov. 1997.

- [17] M.S. Corson, J.P. Maker, and J.H. Cerincione, "Internet-Based Mobile Ad Hoc Networking," *Internet Computing*, pp. 63-70, July-Aug. 1999.
- [18] G.H. Forman and J. Zahorjan, "The Challenges of Mobile Computing," *Computer*, pp. 38-47, Apr. 1994.
- [19] R.G. Gallager, "A Perspective on Multiaccess Channels," *IEEE/ACM Trans. Information Theory*, vol. 31, pp. 124-142, 1985.
- [20] M. Gerla and L. Kleinrock, "Closed Loop Stability Control for S-Aloha Satellite Communications," *Proc. Fifth Data Comm. Symp.*, pp. 210-219, Sept. 1977.
- [21] B. Hajek and T. Van Loon, "Decentralized Dynamic Control of a Multi-Access Broadcast Channel," *IEEE Trans. Automatic Control*, vol. 27, pp. 559-569, 1982.
- [22] J.L. Hammond and P.J.P. O'Reilly, *Performance Analysis of Local Computer Networks*. Addison-Wesley, 1988.
- [23] D.P. Heyman and M.J. Sobel, *Stochastic Models in Operations Research*, vol. I, McGraw-Hill Book Company, 1982.
- [24] R.H. Katz and M. Stemm, "Measuring and Reducing Energy Consumption of the Network Interfaces in Hand-Held Devices," *Proc. Third Int'l Workshop Mobile Multimedia Comm. (MoMuC-3)*, 1996.
- [25] F. Kelly, "Stochastic Models of Computer Communications Systems," *J. Royal Statistical Soc., Series B*, vol. 47, pp. 379-395, 1985.
- [26] L. Kleinrock and F.A. Tobagi, "Packet Switching in Radio Channels: Part I," *IEEE Trans. Comm.*, vol. 23, pp. 1400-1416, 1975.
- [27] R. Kravets and P. Krishnan, "Power Management Techniques for Mobile Communication," *Proc. Fourth Ann. ACM/IEEE Int'l Conf. Mobile Computing and Networking (MOBICOM '98)*, 1998.
- [28] "Part 11: Wireless LAN- Medium Access Control (MAC) and Physical Layer (PHY) Specification," ANSI/IEEE Standard 802.11, Aug. 1999.
- [29] T. Imielinsky and B.R. Badrinath, "Mobile Computing: Solutions and Challenges in Data Management," *Comm. ACM*, Oct. 1994.
- [30] J.P. Monks, V. Bharghavan, and W.W. Hwu, "A Power Controlled Multiple Access Protocol for Wireless Packet Networks," *Proc. Proc. IEEE Ann. Conf. Computer Comm. (Infocom '01)*, Apr. 2001.
- [31] R.L. Rivest, "Network Control by Bayesian Broadcast," *IEEE Trans. Information Theory*, vol. 33, pp. 323-328, 1997.
- [32] W. Stallings, *Local & Metropolitan Area Networks*. Prentice Hall, 1996.
- [33] F.A. Tobagi and L. Kleinrock, "Packet Switching in Radio Channels: Part II," *IEEE Trans. Comm.*, vol. 23, pp. 1417-1433, 1975.
- [34] V.M. Vishnevsky and A.I. Lyakhov, "IEEE 802.11 Wireless LAN: Saturation Throughput Analysis with Seizing Effect Consideration," *Cluster Computing J.*, vol. 5, no. 2, 2002.
- [35] "WaveLAN IEEE 802.11—PC Card User's Guide," User's Guide, Lucent Technologies, 1999.
- [36] J. Weinmiller, H. Woesner, J.P. Ebert, and A. Wolisz, "Analyzing and Tuning the Distributed Coordination Function in the IEEE 802.11 DFWMAC Draft Standard," *Proc. (MASCOT '96)*, Feb. 1996.
- [37] H. Woesner, J.P. Ebert, M. Schlager, and A. Wolisz, "Power-Saving Mechanisms in Emerging Standards for Wireless LANS: The MAC Level Perspective," *IEEE Personal Comm.*, pp. 40-48, 1998.



Raffaele Bruno received the Laurea degree in telecommunications engineering from the University of Pisa, Italy, in 1999. He is currently working toward his PhD degree at the CNUCE Institute of the Italian National Research Council (CNR). His research interests are in the area of wireless and mobile networks with emphasis on efficient wireless MAC protocols, scheduling algorithms for Internet traffic integration, and QoS.



Marco Conti received the Laurea degree in computer science from the University of Pisa, Italy, in 1987. In 1987, he joined the Networks and Distributed Systems Department of CNUCE, an Institute of the Italian National Research Council (CNR) where is currently a senior researcher. His current research interests include Internet architecture and protocols, wireless networks, mobile computing, multimedia systems, and QoS in packet switching networks. He is coauthor of the book *Metropolitan Area Networks* (Springer, London, 1997). He is the technical program chair of the Second IFIP-TC6 Networking Conference "Networking 2002." He served as guest editor for the *Cluster Computing Journal* (special issue on "Mobile Ad Hoc Networking") and *IEEE Transactions on Computers* (special issue on "Quality of Service issues in Internet Web Services"). He was the coordinator for two minitracks ("Mobile Ad Hoc Networking" and "QoS in Web Services") at the Hawaii International Conference on System Sciences (HICSS-34). He is serving as guest editor for *ACM/Kluwer Mobile Networks & Applications Journal* (special issue on "Mobile Ad-hoc Networks"). He is the coordinator of an Exploratory Workshop founded by the European Science Foundation (ESF) on Mobile Ad Hoc Networking. He is member of IFIP WG 6.3, WG 6.8, and the IEEE.



Enrico Gregori received the Laurea degree in electronic engineering from the University of Pisa in 1980. He joined CNUCE, an Institute of the Italian National Research Council (CNR) in 1981. He is currently a CNR research director. In 1986, he held a visiting position at the IBM Research Center in Zurich where he worked on network software engineering and on heterogeneous networking. He has contributed to several national and international projects on computer networking. He has authored a large number of papers in the area of computer networks and has published in international journals and conference proceedings. His current research interests include: wireless access to Internet, Wireless LANS, quality of service in packet-switching networks, energy saving protocols, and evolution of TCP/IP protocols. He is on the editorial board of the *Cluster Computing Journal*. He is member of the IEEE.

► For more information on this or any computing topic, please visit our Digital Library at <http://computer.org/publications/dlib>.